Characterization of the oncogenic functions of Nucleophosmin/NPM1

Nucleophosmin/NPM1 のがん化機能の解明

2016

筑波大学グローバル教育院

School of the Integrative and Global Majors in

University of Tsukuba

PhD program in Human Biology

Jianhuang Lin

Preface

Cancer is the leading cause of death in economically developed countries and the second leading cause of death in developing countries. 12.6% of all deaths are caused by cancer, which is more than the percentage of deaths caused by HIV/AIDS, tuberculosis, and malaria put together. Although earlier detection and more options in treatment have been developed in recent years, the incident rate of cancer continues to increase largely due to the aging and growth of the world population and an increasing adoption of cancer-causing behaviors, particularly smoking, in developing countries. If the trend continues, 15 million people will discover they have cancer in 2020. For the sake of human health, cancer is an urgent global issue needs to be solved.

My scientific interest on cancer research has emerged since the first time I got involved in research when I was an undergraduate student in China, wherein I studied the effect of 5-azacytidine on the inhibition of DNA methylation in mice. After I came to Japan, I was lucky to get the chance to join the Human Biology PhD Program which encourages students to understand and solve the global issues including cancer. Although cancer research is a huge field which many researchers worldwide are working on, I will be happy to be one part of it.

In this dissertation, I focused on the oncogenic functions of a potential oncogenic protein, Nucleophosmin (NPM1). NPM1 is a multi-functional protein that has been involved in various biological processes. my laboratory has contributed to identification of its functions in chromatin remodeling and ribosome biogenesis. Much of the interest in NPM1 has been bolstered by the fact that it is directly implicated in tumorigenesis. However, the mechanism underlying the oncogenic functions of NPM1 remain still poorly understood in spite of the observations that NPM1 overexpression in tumor cells increases cell growth and proliferation, and inhibits cell differentiation and apoptosis. This dissertation describes two projects aimed to contribute to understanding the

mechanism underlying the oncogenic functions of NPM1 in different perspectives. The first project (Chapter 1) entitled “Efficient DNA binding of NF-κB requires the chaperone-like function of NPM1”, revealed the function of NPM1 in NF-κB pathway, an oncogenic pathway plays important roles in both cancer development and inflammation. The second project (Chapter 2) entitled “Functional characterization and efficient detection of Nucleophosmin/NPM1 oligomers”, revealed the function of NPM1 oligomerization for its histone chaperone activity and the dynamic change of NPM1 oligomerization under different cell stimuli. The oligomerization of NPM1 has been suggested to be important for its function in cancer, and that inhibition of NPM1 oligomerization could be the potential approach for cancer therapy.

Table of contents

Chapter 1: Efficient DNA binding of NF-κB requires the chaperone-like function of NPM1

1-1. Abstract

Although NPM1/nucleophosmin is frequently overexpressed in various tumors, the oncogenic role of NPM1 remains unclear. Here I report a new oncogenic role of NPM1 by revealing the link between NPM1 and nuclear factor-κB (NF-κB), a master regulator of inflammation. I found that NPM1 knockdown decreased NF-κB-mediated transcription of selected target genes whose functions enriched in inflammation and immunity by decreasing the recruitment of NF-κB p65 to the gene promoters. NPM1 is directly associated with the DNA binding domain of p65 to enhance its DNA binding activity without being a part of the DNA-NF-κB complex, suggesting the chaperone-like function of NPM1 for NF-kB-mediated transcription. Furthermore, I demonstrated that NPM1 was required for efficient inflammatory gene expression induced by tumor necrosis factor alpha (TNF-α) and lipopolysaccharide in fibroblasts and macrophages. The NF-κB-mediated invasion of breast cancer cells was significantly decreased by NPM1 knockdown. My study suggests a novel mechanistic insight into the NF-κB-mediated transcription and an oncogenic role of NPM1 in both tumor cells and the tumor microenvironment through the regulation of NF-κB.

1-2. Introduction

NPM1 is a highly abundant phosphoprotein that mainly resides in the nucleolus, but continuously moves between the nucleolus, the nucleoplasm, and the cytoplasm (1). My laboratory has identified NPM1 as a factor stimulating adenovirus chromatin remodeling and studied its functions in uninfected cells (2). It is a multifunctional protein involved in various cellular processes such as ribosome biogenesis (3,4), sperm chromatin remodeling (5), centrosome duplication (6), and DNA repair (7). Biochemically, NPM1 shows the histone chaperone activity (8), which is required for the regulation of chromatin structure. Histone chaperones bind directly to histones for their transfer to DNA to assemble chromatin without being incorporated into the chromatin. Most of the interest in NPM1 has been focused on its oncogenic functions. On the one hand, the genetic alterations of the *NPM1* gene have been detected in various hematological malignancies, and strikingly, NPM1 is one of the most frequently mutated genes in acute myeloid leukemia (9). On the other hand, NPM1 is over-expressed in various solid tumors and has been proposed as a tumor marker (10). The expression levels of NPM1 have been reported to be regulated by the oncogene *MYC* (11) and to correlate with tumor recurrence and progression (12). However, the oncogenic functions of NPM1 remain still poorly understood in spite of the observations that NPM1 overexpression in tumor cells increases cell growth and proliferation, and inhibits cell differentiation and apoptosis (10).

A transcription factor, nuclear factor-κB (NF-κB), plays a key role in tumor initiation (13), promotion, progression, and metastasis (14-16). In addition to its oncogenic functions in cancer cells, NF-κB contributes to tumorigenesis through the activation of inflammatory cells in the tumor microenvironment because of its central role in the immune system. Therefore, NF-κB has been suggested to be a key link between inflammation and cancer. NF-κB was

originally discovered as a site-specific DNA-binding protein complex that binds to the enhancer element of the immunoglobulin (Ig) kappa light-chain of activated B cells (17). The mammalian NF-κB family contains the following five proteins: 1) p65 (RelA); 2) c-Rel; 3) RelB; 4) p50; and 5) p52, which function as homo- or hetero-dimers to control gene transcription (18). The most abundant form of the NF-κB complex contains the p65–p50 heterodimer that regulates the genes including those for cytokines, chemokines, adhesion molecules, and enzymes that produce secondary inflammatory mediators.

Achieving precise and sufficient gene regulation by NF-κB requires specific posttranslational modifications and interactions with cofactors (19). Indeed, it was predicted that the original size of the native NF-κB complex from nuclear extracts is much larger than that of the NF-κB p65–p50 heterodimer. Moreover, the native NF-κB complexes have a higher affinity for the Ig κB DNA motif than the reconstituted p65–p50 heterodimer does (20,21), which highlights the importance of cofactors for NF-κB DNA binding. It has been reported that ribosomal protein S3 (22), Sam68 (23), telomerase (24), and cyclin dependent kinase 6 (25) directly associate with the NF-κB complex and enhance its DNA binding activity.

It was also observed that a nucleolar protein nucleophosmin/B23/NPM1 interacts with NF-κB and regulates the expression of the *SOD2* gene (26), however, whether NPM1 regulates the NF-κB pathway and the effect of NPM1 on NF-κB-mediated transcriptome are still unknown. In this study, I aimed to reveal the role of NPM1 in the NF-κB pathway and its effect on NF-kB-mediated transcriptome. My findings are important for two main reasons: 1) NF-κB, a master regulator of inflammation, requires the chaperone-like activity of an oncogenic protein NPM1 for its functions and; 2) two oncogenic factors, NPM1 and NF-κB, are suggested to cooperatively regulate tumor progression through cancer cells and the tumor microenvironment.

1-3. Materials and Methods

1-3-1. Plasmid constructs

Plasmids pET-14b-B23.1, pGEX2T-B23.1, pGEX2T-B23.2, pGEX2T-B23.3, pGEX2T-B23.1-CR and pGEX2T-B23.1-ΔA1A2 have been described previously (27). To construct pGEX2T-B23.1-ΔN, B23.1-ΔN fragment was cut out from template plasmid pET14b-B23.1-ΔN (27) by BamH I and cloned into the same site of pGEX2T vector. The p65/RelA, RelB, c-Rel, and p50 genes were cloned by PCR using primer sets 5'-ATGCGGATCCATGGACGAACTGTTCCCCCT-3' and 5'-ATGCGGGATCCTTAGGAGCTGATCTGACTCA-3', 5'-AAAGAATTCATGCTTCGGTCTGGGCCAGC-3' and 5'-AAAGAATTCCTACGTGGCTTCAGGCCCCG-3', 5'-AAAGGATTCATGGCCTCCGGTGCGTATAA -3' and 5'-AAAGAATTCTTATACTTGAAAAAATTCAT -3', and 5'-AAAGAATTCATGGCAGAAGATGATCCATA-3' and 5'-AAACTCGAGTAGGTTCCATGCTTCATCCCAG-3', respectively. The amplified p65, RelB, c-Rel, and p50 cDNA fragments were subcloned into the BamH I-digested, EcoR I-digested, BamH I and Eco RI-digested, and EcoR I and Xho I digested pcDNA3.1-Flag vector. The p65 and p50 cDNAs were also cloned into pcDNA3-HA vector. To construct vectors expressing p65 deletion mutants, deletion mutant fragments were cloned by PCR using primers 5'-ATGCGGATCCATGGACGAACTGTTCCCCCT-3' and 5'-AAAGGATCCTTAAGAAAGGACAGGCGGCAGGC-3' for p65-N1 (a.a.1–180), 5'-AAAGGATCCCATCCCATCTTTGACAATCG-3' and 5'-AAAGGATCCTTAAGAAGCTGAGCTGCGGGAAG-3' for p65-N2 (a.a.181–340), 5'-AAAGGATCCGTCCCCAAGCCAGCACCCCA-3' and 5'-ATGCGGGATCCTTAGGAGCTGATCTGACTCA-3' for p65-C (a.a. 341-551), p65 forward primer and p65-N2 reverse primer for p65-N (a.a.1–340), p65-N2 forward and p65 reverse primers for p65-N2C (a.a.181–551), the amplified

cDNAs were subcloned into the BamH I sites of pcDNA3.1-Flag and pET14b vectors. All the plasmids were confirmed by DNA sequencing.

1-3-2. Animals, cell culture, transfection, and reagents

C57BL/6J-*Apc*$^{Min/+}$ mice were purchased from the Jackson Laboratory. The *Min* pedigree was maintained by mating C57BL/6J wild type females with C57BL/6J-*Apc*$^{Min/+}$ males, genotype analysis was performed using a PCR assay as described (28). Colon adenomas were developed by administration of 2% Dextran Sulfate Salt in drinking water for 7 days during 5th week of age. Mice were sacrificed at 8 weeks of age and subjected to histological analyses. BDF-1 mice were purchased from CLEA Japan, Inc. HeLa, HEK293T, BT-20, MDA-MB-157, MDA-MB-231, MDA-MB-436 cells, and *p53*$^{-/-}$ and *p53*$^{-/-}$NPM1$^{-/-}$ mouse embryonic fibroblast (MEF) cells were cultured in DMEM supplemented with 10% heat-inactivated fetal bovine serum (FBS) at 37℃ with 5% CO_2. Primary macrophages were prepared from wild type BDF-1 mice (10-week old) injected with 3.84% (w/v) thioglycollate 3 d after injection. PBS (5 ml) was injected into peritoneal cavity and recovered. Cells were centrifuged and seeded in RPMI1640 medium (GIBCO) supplemented with 10% FBS, and incubated at 37ºC for 0.5 h. Non-adherent cells were removed by wash with PBS, and cells were maintained in the same medium.

1-3-3. Transfection and reagents

Transfection of plasmid DNA and siRNAs were performed by GeneJuice (Novagen) and Lipofectamine RNAiMAX (Life technologies), respectively, according to the manufacturer's instructions. Stealth RNAs for negative controls and human NPM1 were described previously (29). Mouse NPM1 (siRNA ID: s124573) and human NF-κB p65 (HSS109159) were obtained from Life technologies. Antibodies used were NPM1 (Invitrogen), Flag tag (M2, Sigma Aldrich), p65 (ab7970, Abcam), I-κBα (sc-371, Santa Cruz), and β-actin

(sc-47778, Santa Cruz). Recombinant human TNF-α (PEPROTECH) and Lipopolysaccharide (LPS) (Sigma) were commercially available.

1-3-4. Preparation of proteins

Purifications of GST-tagged proteins and his-tagged proteins were described previously (30). For purification of Flag-tagged proteins, HEK 293T cells transfected with appropriate expression vectors were suspended in buffer A (0.1% Triton X-100, 20 mM Tris-HCl pH7.9, 10 mM KCl, 1.5 mM $MgCl_2$, 0.5 mM PMSF) containing 400 mM NaCl on ice for 10 min and rotate at 4ºC for 30 min followed by centrifuge at 15k rpm, 4ºC for 15 min. The supernatants were recovered and diluted with twice volumes of buffer A without NaCl. The cell extracts were incubated with anti-Flag M2 affinity gels (SIGMA–ALDRICH) for 2 h at 4ºC and then washed by buffer B (0.1% Triton X-100, 50 mM Tris-HCl pH7.9, 0.5 mM PMSF) containing 300 mM NaCl. The proteins bound with the resin were eluted with buffer A containing 150 mM NaCl and Flag peptide (SIGMA–ALDRICH), dialyzed against buffer H (20 mM Hepes–NaOH pH 7.9, 50 mM NaCl, 0.5 mM EDTA, 1 mM DTT, 0.1 mM PMSF and 10% Glycerol).

1-3-5. Immunoprecipitation and GST-pull down assay

HEK293T cells transfected with the expression vectors for Flag-p65, Flag-p50, HA-p65 or Flag-p65 deletion mutants were sonicated in buffer B containing 150 mM NaCl. The cell lysates were incubated with anti-Flag M2 affinity gels (SIGMA–ALDRICH) in buffer A for 1 h at 4ºC, and the resins were then washed with the same buffer. The proteins bound with the resin were eluted with buffer B containing Flag peptide (SIGMA–ALDRICH), separated by SDS-PAGE and detected by western blotting. For GST-pull down assays, GST, GST-NPM1 or GST-NPM1 deletion mutants was incubated with glutathione-sepharose beads in buffer A for 45 min and washed with buffer A twice. The beads were mixed with Flag-p65, RelB, or c-Rel and incubated at 4℃ for 2 h followed by

extensive washing with the same buffer. Proteins were eluted from the beads by a SDS sample buffer, separated by SDS-PAGE, and visualized by CBB staining and western blotting.

1-3-6. Reporter assay

HeLa cells ($3x10^4$ per well) were seeded in 24-well plates and transfected with 80 ng of pNF-κB-TA-Luc (Firefly luciferase) and 20 ng of pTA-RL (*Renilla* luciferase) at 48 h after transfection with siRNA for NPM1 or negative control. Sixteen hours after transfection, cells were treated with 20 ng/ml TNF-α for different time courses as described in the legend. Luciferase assay was performed using *Renilla* Luciferase Assay System kit (Promega Corporation, USA) according to the manufacturer's instructions. The sane experiments were performed with *p53*$^{-/-}$ and *p53*$^{-/-}$*NPM1*$^{-/-}$ MEFs.

1-3-7. RT-qPCR

Total RNA was extracted using RNeasy Kit (Qiagen) according to the manufacturer's instructions. cDNA was prepared from purified RNA (1 μg) by using ReverTraAce (Toyobo) with oligo dT primer. Real-time PCR was carried out in triplicate with primers (sequences are shown in Table S1) by using SYBR Green Realtime PCR Master Mix-Plus (Toyobo) in the Thermal Cycler Dice Real-Time PCR system (TaKaRa).

1-3-8. Chromatin Immunoprecipitation (ChIP)

ChIP was performed with HeLa cells treated with or without TNF-α. Cells were fixed with 1.4% formaldehyde at room temperature for 10 min, the whole cell lysates were sonicated to generate DNA fragments 200–1000 base pairs in length. The sonicated lysates were used for ChIP with anti-p65, anti-NPM1 or IgG control antibodies. After washing, the complexes were eluted, protein-DNA crosslink was reversed, and DNA was purified and used for quantitative PCR.

Primer sequences used for PCR were shown in Table S2.

1-3-9. EMSA

Radio-labeled double-stranded oligonucleotide probes wt Ig κB (5'-AGTTGAGGGGACTTTTCCCAGG-3') and mutant Ig κB (5'-AGTTGAATCCACTTTCCCAGG-3') were used for EMSA. EMSA was carried out as previously described (22). Briefly, p65 or p50 protein (20 ng/sample) was incubated with the purified GST, GST-NPM1, or His-NPM1 protein at 25℃ for 30 min, followed by additional incubation with [^{32}P]-labeled Ig κB (WT) or Ig κB (Mut) oligonucleotide at 25℃ for 30 min. Samples were resolved on a 6% native PAGE in 0.5xTBE buffer. For supershift analyses, recombinant proteins were preincubated with 0.2 μg of antibodies for 20 min on ice prior to the addition of labeled probes.

1-3-10. Immunofluorescence and Proximity Ligation Assays

Cells on cover slips were fixed with 3% paraformardehyde in PBS, and permeabilized in PBS containing 0.5% Triton X-100. The cells on coverslips were then incubated with anti-NPM1 and p65 antibodies diluted with PBS containing 0.5% non-fat dry milk. Localization of proteins was visualized with secondary antibodies conjugating with AlexaFluor dyes (Molecular Probes). During final wash with PBS containing 0.1% Triton X-100, DAPI DNA staining dye was added and incubated for 15 min at room temperature. *In situ* proximity ligation assay (PLA) kit (Sigma-ALDRICH) was used to detect protein-protein interaction in fixed cells according to the manufacturer's instructions. PLA signals were quantitatively analyzed by the image processing software Imaris (Carl Zeiss microimagining). Localization of proteins, DNA, and PLA signals was observed under confocal microscope (LSM EXCITER; Carl Zeiss Microimaging, Inc.).

1-3-11. Microarray hybridization and data analysis

HeLa cells were incubated with NPM1 or control siRNA for 72 h and treated without or with 20 ng/ml TNF-α for 2 h. Total RNA was then isolated using RNeasy Kit (Qiagen) according to the manufacturer's instructions. The sense-strand cDNA was prepared using Ambion WT Expression Kit from 200 ng total RNA. The cDNA was then fragmented and labeled using the Affymetrix GeneChip WT Terminal Labeling Kit. The fragmented and labeled cDNA was injected to the Gene Arrays 1.0 ST and incubated at 45ºC with 60 rpm for 17 hr. The hybridized samples were washed and stained using Affymetrix fluidics station 450. GeneChips were scanned using Affymetrix GeneArray Scanner 3000 7G Plus. All kits were obtained from Affymetrix (Santa Clara, CA) and experiments were performed according to the manuals. Raw data were analyzed using the rma() function in R-Bioconductor (31) package "affy" (32,33) with default setting. Background correcting was processed by the RMA (robust multichip averaging) (34), the data were normalized by quantiles, and the signal intensity of each probe set was obtained by the method medianpolish. The annotation of probe sets was performed by Bioconductor hugene10sttranscriptcluster.db. The microarray data are available at the NCBI Gene Expression Omnibus (GEO) under accession number GSE81785. Gene ontology analysis was performed using DAVID (The Database for Annotation, Visualization and Integrated Discovery) (http://david.abcc.ncifcrf.gov/) (35,36).

1-3-12. Immunohistochemistry (IHC)

Apc$^{min/+}$ mice (12-weeks old) were given 2% (w/v) DSS in drinking water for 1 week, then changed to normal drinking water for 2 weeks. Colon tissues from the mice were cut and opened, fixed in phosphate-buffered 10% formalin and embedded in paraffin and cut into 5-μm sections. The sections were dewaxed, rehydrated, and immersed in 3% hydrogen peroxide for 20 minutes to quench endogenous peroxidase activity. Antigen retrieval was performed at 95ºC for 20 minutes in sodium citrate buffer (pH 6.0). The sections were incubated with

blocking buffer (PBS supplemented with 2% goat serum and 1% bovine serum albumin) for 1 hour, anti-NPM1 or p65 antibodies for 1 hour at RT, a biotinylated secondary antibody for 45 min, and peroxidase-conjugated streptavidin solution for 45 min. Protein localization was visualized with 3, 3-diaminobenzidine and sections were lightly counterstained using Gill's haematoxylin.

1-3-13. Matri-gel invasion assay

Invasion assays were performed using transwell chambers (24-well insert; pore size, 8 μm; Corning-Costar, Corning, NY, USA). Transwell membrane was coated with 30 μg of matrigel and incubated at 37ºC for 3 h. MDA-MB-231 cells ($5x10^4$) in 200 μl of serum-free medium were seeded into the upper chamber of the transwell and medium supplemented with serum was used as a chemoattractant in the lower chamber. The cells on the upper chamber were treated with or without TNF-α, incubated for 16 h, and cells that did not invade through the pores were removed with a cotton swab. Cells on the lower surface of the membrane were fixed with methanol and stained with 0.05% crystal violet. The stained cells were counted under a microscope (Leica Dmi8) in 3 random fields/well.

1-4. Results

1-4-1. Interaction between NPM1 and NF-κB

A previous study showed that NPM1 interacts with the NF-κB subunits p65 and p50 (26). However, whether NPM1 also interacts with other NF-κB family proteins and the interaction is direct or not have never been examined. I first examined the interaction between NPM1 and the NF-κB family Rel proteins, p65 (RelA), RelB, and c-Rel. Flag-tagged p65, RelB, and c-Rel were purified (Fig. 1A) and a glutathione S-transferase (GST) pull down assay was performed. All Flag-tagged p65, RelB, and c-Rel were more efficiently precipitated with GST-NPM1 than GST. Flag-p65 precipitated by GST-NPM1 was much more efficient than Flag-RelB and Flag-c-Rel (Fig. 1B), suggesting that NPM1 preferentially associates with p65. I next confirmed the interaction between NPM1 and the classic NF-κB complex proteins p65 and p50 by co-immunoprecipitation with the exogenous Flag-tagged NF-κB proteins. NPM1 was co-immunoprecipitated with both Flag-p65 and Flag-p50 (Fig. 1C, lanes 6–7). When Flag-p50 and HA-p65 were co-expressed and immunoprecipitated with anti-Flag antibody, HA-p65 and NPM1 were immunoprecipitated with Flag-p50 (lane 8). I also found that NPM1 directly interacted with p65 and p50 with similar efficiency (Fig. 1D). Furthermore, *in situ* proximity ligation assay (PLA) using antibodies for both NPM1 and p65 revealed that NPM1 interacted with p65 mainly in the nucleus (Fig. 1E, top panels). Treatment of cells with TNF-α, which activates the NF-κB pathway, dramatically enhanced the interaction (Fig. 1E, bottom panel and Fig. 1F). The PLA signals were mainly detected in the nucleoplasm, indicating that this is where the interaction between p65 and NPM1 occurred. Because NPM1 is mainly localized in the nucleolus, we tested whether NPM1 localization was changed upon treatment of cells with TNF-α. HeLa cells stably expressing enhanced green fluorescent protein (EGFP)-NPM1 were treated with TNF-α and the localizations of p65 and EGFP-NPM1 were examined (Fig. 1G). p65 was translocated to the nuclei 15 min after TNF-α treatment. I found that

although the interaction between p65 and NPM1 occurred in the nucleoplasm (Figs. 1E and F), TNF-α treatment did not clearly change the localization of EGFP-NPM1.

1-4-2. NPM1 regulates NF-κB-dependent gene transcription

I next examined the effect of RNAi-mediated knockdown of NPM1 on the expression of NF-κB-dependent reporter gene expression in HeLa cells. NPM1 siRNA significantly decreased the total amount of NPM1 compared with the nonspecific (NS) control siRNA (Fig. 2A). The reporter activity was found to be decreased by NPM1 knockdown even in the absence of TNF-α. As expected, TNF-α treatment induced the NF-κB-driven luciferase activity in NS siRNA-treated cells, but this induction was significantly decreased in NPM1 siRNA-treated cells (Fig. 2B).

I performed microarray analysis to comprehensively analyze the effect of NPM1 knockdown on the NF-κB-dependent gene expression induced by TNF-α treatment in HeLa cells. I found that without TNF-α treatment, 288 genes were up-regulated (>1.5-fold) and 359 genes were down-regulated (<0.667-fold) by NPM1 knockdown (Fig. 2D), suggesting that NPM1 is involved in the regulation of a variety of genes. Upon stimulation with TNF-α, 77 genes were up-regulated (>1.5-fold) and 13 genes were down -regulated (<0.667-fold) (Fig. 2C). In addition, in TNF-α treated cells, NPM1 knockdown decreased the expression of 445 genes (<0.667-fold) and increased the expression of 223 genes (>1.5-fold) (Fig. 2E). Among the 77 genes up-regulated by TNF-α treatment, 32 genes were down-regulated (>1.5-fold) by NPM1 knockdown (Fig. 2F, upper panel) and only two genes were up-regulated (>1.5-fold) by NPM1 knockdown. When the cutoff fold-change (chip2 vs chip4) was set to 1.2, the number of the genes down- regulated by NPM1 knockdown was increased to 55, while only seven genes were up-regulated (>1.2-fold) by NPM1 knockdown (Fig. 2I). These results suggested that NPM1 is involved in the

regulation of most, but not all, genes stimulated by TNF-α treatment. The heat map shows the expression of the 32 genes sorted by the fold change values (Figs. 2G and 2H) between control and NPM1 knockdown in TNF-α-treated cells. Many of them are cytokines, such as *IL-8*, *TNF-α*, and *IL-6*. Indeed, gene ontology (GO) analysis of the 32 TNF-α-induced genes whose expressions were down-regulated (>1.5-fold) by knockdown of NPM1 showed functional enrichment in inflammation and immunity such as cytokine activity, cytokine, inflammatory response, response to wounding, and defense response (Fig. 2F, lower panel). To confirm the microarray analyses, reverse transcriptase-mediated polymerase chain reaction (RT-PCR) was performed (Fig. 2J). The expressions of eight genes (*IGFL1*, *SELE*, *CCL2*, *RND1*, *PLAU*, *IL-8*, *TNF-α*, and *CCL20*) were confirmed to be significantly reduced by NPM1 knockdown. In addition, I confirmed that the expression levels of *NR4A2* and *DUSP5* were slightly increased by NPM1 knockdown. It should be noted that the increase or decrease of those genes was observed even in the absence of TNF-α treatment.

To explore the mechanism by which NPM1 regulates the expression of the genes stimulated by TNF-α, I examined whether NPM1 knockdown affected the NF-κB signaling pathway such as I-κB protein degradation, NF-κB nuclear translocation, and NF-κB recruitment to its target genes upon stimulation by TNF-α. The I-κB proteins bind NF-κB to retain it in the cytoplasm and are quickly degraded upon stimulation by TNF-α through the ubiquitin-proteasome system to allow the nuclear translocation of NF-κB. The *I-κB* genes are target genes of the NF-κB complex and the I-κB–NF-κB complex constitutes a feedback oscillatory circuit (37). Indeed, I-κBα was quickly degraded upon TNF-α treatment and the expression was recovered within 60 min, and the oscillatory expression was observed with peak expressions at 60 min and 105 min (Fig. 3A). I found that I-κBα protein degradation was similarly observed 15 min after TNF-α stimulation regardless of the level of NPM1 expression (Fig.

3A, lane 2). However, the pattern of oscillatory expression of I-κBα was changed by NPM1 knockdown, suggesting that NPM1 is involved in the I-κBα expression. Likewise, the nuclear translocation of NF-κB p65 upon TNF-α treatment was not affected by knockdown of NPM1 (Fig. 3B). I then examined whether NPM1 affected the binding of NF-κB to target gene promoters by chromatin immunoprecipitation (ChIP). In unstimulated cells, a low but distinct amount of p65 was detected at the promoter regions of *TNF-α*, *PLAU*, *IL-8*, *NR4A2*, and *DUSP5* genes. Upon stimulation with TNF-α, the binding of p65 to these genes was significantly increased. However, NPM1 knockdown decreased the p65 binding to the *TNF-α*, *PLAU*, and *IL-8* gene promoters in both unstimulated and TNF-α-stimulated cells. In contrast, the recruitment of p65 to the promoter regions of *NR4A2* and *DUSP5* was not affected by knockdown of NPM1 (Fig. 3C). These results indicate that NPM1 stimulates the binding of NF-κB to a subset of NF-κB target gene promoters. I noted that the expression of *NR4A2* and *DUSP5* was increased by NPM1 knockdown regardless of TNF-α treatment (Fig. 2J), whereas the promoter binding of p65 to these genes was not significantly affected. These results indicate that NPM1 suppresses these genes independent of the promoter binding of NF-κB.

1-4-3. NPM1 enhances the DNA binding activity of NF-κB

Considering the effect of NPM1 on the binding of NF-κB to target gene promoters *in vivo* and its direct interaction with NF-κB *in vitro*, I next examined whether NPM1 affected the binding of NF-κB to the κB site *in vitro* by the electrophoretic mobility shift assay (EMSA) using purified recombinant NF-κB proteins and His-NPM1 (Fig. 4A). When either Flag-p65 or Flag-p50 was expressed, a homo-dimer of Flag-tagged proteins and a minor population of a heterodimer of Flag-tagged proteins and endogenous p65 or p50 were purified (Fig. 4A, lanes 2 and 3). When Flag-p50 and HA-p65 were co-expressed and purified with anti-Flag affinity gel, the Flag-p50 homodimer and the

heterodimer of Flag-p50 and HA-p65 were purified (Fig. 4A, lane 4). All purified p50 homodimer, p65 homodimer, and p65-p50 heterodimers specifically bound to the κB oligonucleotide (Fig. 4B, lanes 2 and 5), but not to the mutant κB oligonucleotide (lanes 3 and 6). The addition of anti-p65, anti-Flag tag, or anti-HA tag antibody induced supershift, thereby ensuring the binding of specific NF-κB dimers to the κB oligonucleotide (lanes 4 and 7–9). NPM1 significantly increased the binding of all NF-κB dimers to the κB oligonucelotide in a dose dependent manner (Fig. 4C), whereas NPM1 itself did not bind to the κB oligonucleotide (Fig. 4C, lane 1).

To test whether NPM1 is included in the NF-κB/DNA complex, EMSA with or without anti-NPM1 was performed (Fig. 4D). The Flag-p65 homodimer and Flag-p50–HA-p65 heterodimers were bound to the κB oligonucleotide, which was enhanced by NPM1 (Fig. 4D, lanes 2, 3, 6, and 7). The addition of Flag antibody, but not NPM1 antibody, induced a supershift of the complex containing DNA and the NF-κB proteins (Fig. 4D, lanes 4, 5, 8 and 9). Considered together, these results indicated that NPM1 binds directly to and enhances the DNA binding activity of the NF-κB proteins without being incorporated into the NF-κB/DNA complex.

To further explore whether NPM1 is incorporated into the NF-κB/DNA complex *in vivo*, I next performed ChIP assays with antibodies against endogenous p65 and NPM1 (Fig. 4E). The binding of p65 to the *PLAU* and *IL-8* gene promoters, but not to the *ribosome RNA* gene (rDNA), was increased upon TNF-α treatment in a time-dependent manner. NPM1 showed constant binding to rDNA as previously reported (3), but was not recruited to the *PLAU* and *IL-8* gene promoters during the entire time course after TNF-α treatment. These results support my conclusion that NPM1 is not included in the NF-κB/DNA complex.

1-4-4. NPM1 and κB DNA compete for binding to NF-κB

I next attempted to clarify the mechanism by which NPM1 enhances the DNA binding activity of NF-κB. To this end, we first determined the NF-κB binding domain of NPM1 by a GST-pull down assay with the NPM1 deletion mutant proteins (Fig. 5A). A splicing variant of NPM1/B23.1 termed B23.2 that lacks the C-terminal RNA binding domain interacted with p65, indicating that the C-terminal RNA binding domain is dispensable for p65 binding (Fig. 5B, lane 7). Further analyses suggested that the N-terminal oligomerization domain and acidic regions were also dispensable for p65 binding and the C-terminal region termed NPM1-CR was sufficient to interact with p65 *in vitro* (Fig. 5B, lanes 2–6).

Next, the NPM1 binding domain of p65 was determined by immunoprecipitation assay. Flag-tagged p65 proteins were expressed in 293T cells and immunoprecipitated with anti-Flag antibody followed by western blotting with anti-NPM1 antibody (Figs. 5C and D). Consistent with the data shown in Fig. 1C, NPM1 was co-precipitated with full length p65. The N-terminal domain of p65 (p65-N1) that contains the DNA binding domain of p65, but not the dimer formation domain without or with the activation domain (p65-N2 or p65-N2C, respectively), co-precipitated with endogenous NPM1. The N-terminal domain with the dimer formation domain (p65-N) also efficiently co-precipitated NPM1, indicating that NPM1 interacts with the DNA binding domain of p65.

Because NPM1 interacts with the DNA binding domain, I next questioned whether the N-terminal domain is sufficient for NPM1 to enhance the DNA binding activity of p65. NPM1 increased the binding of p65-N to the κB DNA in a dose dependent manner (Figs. 6A and B), suggesting that the C-terminal activation domain of p65 is dispensable for NPM1 to enhance the DNA binding activity of p65.

Given that NPM1 directly interacted with the DNA binding domain of p65 and that NPM1 was not incorporated into the NF-κB/DNA complex, it was speculated that NPM1 and DNA compete for the binding to NF-κB. This speculation was first examined by gel shift assay using purified p65-N and NPM1 (Fig. 6C). NPM1 is an acidic protein and migrated to the cathode in native gel, whereas p65-N entered the

gel inefficiently (lanes 1 and 2). The mobility of NPM1 was shifted upon addition of p65-N in a dose dependent manner (lanes 2–5). However, the addition of κB DNA increased free NPM1 and the DNA-p65-N complex appeared (lanes 6–8). Taken together, these results suggest that the chaperone-like function of NPM1 is required for the efficient DNA binding of NF-κB. To further confirm this conclusion, disruption of NPM1-p65-N complex by the κB DNA oligonucleotide was examined using purified proteins and oligonucleotide (Fig. S4). The p65-N protein bound to GST-NPM1 was eluted in the supernatant in an oligonucleotide concentration-dependent manner. Because the mutant κB DNA did not efficiently compete with NPM1 for the binding to p65-N, NPM1 transferred the p65-N protein preferentially to the κB DNA.

To clarify the mechanism by which NPM1 regulates a subset of NF-κB target genes, EMSA assays were performed using the κB site DNA fragments derived from *Ig*, *IL-8*, and *NR4A2* genes (Fig. 6D). The p65-N protein bound to all three κB site DNAs with similar efficiency. Interestingly, NPM1 significantly enhanced the binding of p65 to *Ig* and *IL-8* κB sites, whereas the effect of NPM1 on the binding of p65-N to the *NR4A2* κB site was very low (Fig. 6E). This result indicates that the κB sequence or the sequence around it determines the requirement of NPM1 for the efficient p65 binding to its target sites.

1-4-5. NPM1 abrogates the intramolecular interaction of p65

It was previously reported that the intramolecular interaction between the N- and C-terminal domains of p65 blocks the binding of CBP/p300 to the p65 protein (38). This suggests that the formation of the transcription activation complex is controlled by the intramolecular interaction of p65. Considering that NPM1 interacts with the N-terminal domain of p65, I speculated that NPM1 might compete with the C-terminal domain of p65 for the binding to the N-terminal domain of p65, thus blocks the intramolecular interaction of p65 to enhance the assembly of the transcription activation complexes. To examine this, gel shift assay was performed using purified NPM1, p65-N, and p65-C

(Fig. 7A). Free p65-C migrated to the cathode and the p65-C band was shifted upon addition of p65-N in its dose-dependent manner (lane 2–5), ensuring the interaction between p65-N and p65-C. Interestingly, the addition of NPM1 increased free p65-C (lanes 6–8) and the NPM1-p65-N complex appeared, indicating that NPM1 abrogates the intramolecular interaction between p65-N and -C. From these results, it is suggested that the p65 subunit of NF-κB translocated to the nuclei upon various stimuli is bound by NPM1. NPM1 enhances the DNA binding of NF-κB via its chaperone-like function and simultaneously abrogates the intramolecular interaction of p65 to enhance the assembly of the transcription activation complexes (Fig. 7B).

1-4-6. Functional intersection between NPM1 and NF-κB

Because NF-κB is a crucial regulator of tumor formation, progression, and migration (39), and NPM1 is highly expressed in cancer cells (10), I next investigated the biological significance of the interaction between NF-κB and NPM1 in cancer. I first examined the expression of NPM1 and NF-κB in normal colon and adenomas obtained from multiple intestinal neoplasia (min) mice carrying a mutation in the *adenomatous polyposis coli* gene (*Apc*$^{min/+}$ mice) treated with dextran sodium sulfate, an inducer of colitis (Fig. 8A). The normal colon epithelium (Fig. 8A, lower section of the pictures) showed uniform crypts, whereas the crypt structures were disorganized in the adenomas (upper section of the pictures). Hematoxylin and eosin (HE) staining clearly demonstrated that the cells in adenomas exhibited slightly larger nuclei, prominent nucleoli, and intensely colored cytoplasm. I found that much stronger expression of both the p65 subunit of NF-κB and NPM1 was detected in adenomas than in normal colon. Both proteins were also detected at high levels in stromal cells. Importantly, p65 was mainly detected in the nucleus in stromal cells in adenomas, suggesting that NF-κB was activated in stromal cells. Given that tumor cells are associated with a heterogeneous mixture of

stromal cells that include fibroblasts and immune cells, it was possible that NPM1 and NF-κB cooperatively induce cancer progression by the functions of stromal cells. To examine this possibility, I tested the functional interaction between NPM1 and NF-κB in both mouse embryonic fibroblasts (MEFs) and peritoneal macrophages. I used *p53*$^{-/-}$ and *p53*$^{-/-}$*NPM1*$^{-/-}$ MEFs to examine the effect of NPM1 depletion on the NF-κB-driven luciferase expression. *NPM1*$^{-/-}$ MEFs undergo cell cycle arrest due to p53 activation and can grow only when p53 is also depleted (40). Consistent with the results in HeLa cells, both TNF-α and LPS stimuli induced the NF-κB-driven luciferase activity in *p53*$^{-/-}$ control MEFs (Fig. 8C). However, the reporter activities induced by both stimuli were significantly lower in *p53*$^{-/-}$*NPM1*$^{-/-}$ MEFs than those in *p53*$^{-/-}$ control MEFs (Fig. 8C). Next, mouse peritoneal macrophages were treated with control or NPM1 siRNAs and the expression of NPM1 was examined by western blotting (Fig. 8D). NPM1 expression was clearly decreased by NPM1 siRNA treatment, whereas that of actin was unchanged. The expressions of NF-κB target genes *TNF-α*, *IL-1β*, *IL-6*, and *IFN-β*, but not *GAPDH*, were significantly induced by LPS (Fig. 8E, lanes 1 and 2). The induced expressions of *TNF-α*, *IL-1β*, and *IFN-β* were significantly decreased by NPM1 knockdown, whereas the expression of the *IL-6* gene was not significantly affected. Considered together, my results demonstrated that NPM1 and NF-κB cooperatively regulate the inflammatory responses both in fibroblasts and macrophages.

I next examined the functions of the NPM1-NF-κB complex in cancer cells. The expression level of NPM1 in various breast cancer cell lines were examined using the GOBO database (41), because breast cancer cells having ‘triple negative’ phenotype, namely no expression of estrogen receptor, progesterone receptor, and ERBB2, show constitutive activation of the NF-κB activity (42). Previous study showed that NPM1 is highly expressed in normal luminal epithelial cells and its expression is induced by hormones (43). However, among commonly used 51 breast cancer cell lines, the expression of

NPM1 was highest in the basal B subtype cell lines that show ‘triple negative’ phenotype and exhibit a stem cell-like gene expression profile (44), and was the lowest in luminal subtype cell lines that show more differentiated and non invasive phenotype (Figs. 9A and 9B) (44). To confirm the expression of NPM1 in basal A- or B-type breast cancer cell lines (BT20, MDA-MB-157, MDA-MB-231, and MDA-MB-436), RT-PCR and western blotting were performed (Fig. 8F). The results indicated that the expression of NPM1 was the highest in MDA-MB436 cells among the 4 cell lines tested. The previously determined constitutive NF-κB activity of these cells (42) were plotted against NPM1 mRNA level (Fig. 8G). The constitutive NF-κB activity was correlated with the expression level of NPM1, although the expression level of p65 was not very high in MDA-MB-436 cells (Figs. 8H and G). These results support the idea that NPM1 is a positive regulator of the NF-κB complex.

Because NF-κB has been reported to regulate cancer cell migration and invasion (39), I examined the effect of NPM1 knockdown on TNF-α-induced cancer cell invasion by matrigel invasion assays using a breast cancer cell line, MDA-MB-231 (Figs. 10B and 8H). I demonstrated that TNF-α treatment significantly enhanced the invasion of MDA-MB-231 cells. Upon knockdown of NF-κB p65, the TNF-α induced invasion of MDA-MB-231 cells was greatly reduced, indicating that the invasion enhanced by TNF-α was NF-κB-dependent. Knockdown of NPM1 or double knockdown of NPM1 and p65 both blocked the TNF-α induced invasion, suggesting that NPM1 regulates cancer cell invasion through enhancing NF-κB signaling. The expression level of p65 and NPM1 by siRNA treatment was confirmed by western blotting (Fig. 10A). From the TNF-α induced genes that were down-regulated by NPM1 knockdown as shown in the heatmap (Fig. 2D), I picked up and examined the expression of the cytokines CCL2 and CCL20, which have been reported to regulate the migration of breast cancer cells (45,46). Consistent with the invasion assays, p65 knockdown efficiently

blocked the expression of its target genes *CCL2* and *CCL20*, but not *GAPDH*, and NPM1 knockdown also decreased the target gene expression (Fig. S5C). Considered together, I concluded that NPM1 and NF-κB cooperatively regulate the cancer progression induced by the NF-κB signaling.

1-5. Discussion

The data presented in this study suggest a working model in which NPM1 interacts with NF-κB in the nucleus to stimulate the binding of NF-κB to target gene promoters. Interestingly, NPM1 itself disassociates from NF-κB once NF-κB binds to DNA (Fig. 7B). NPM1 interacts with the N-terminal DNA binding domain of p65 and competes with DNA for the binding to p65, which results in the release of NPM1 after p65 binds to DNA (Fig. 6). These results suggest that the chaperone-like function of NPM1 is required for the maximal transcription stimulatory activity of NF-κB. Another contribution of NPM1 on NF-κB mediated transcription could be explained by the result that inhibits the intramolecular interaction between the N- and C-terminal domains of p65 (Fig. 7A) to allow transcriptional coactivators CBP/p300 to interact with p65-C terminus because the p65-N/p65-C intramolecular interaction blocks the p65-C binding site of CBP/p300 (38). I noted that although the expressions of some NF-κB target genes such as *PLAU* and *IL-8* were greatly decreased by NPM1 knockdown (Fig. 2E), the recruitment of NF-κB p65 to the promoters was only decreased to about half (Fig. 3C). Thus, it is possible that NPM1 regulates both the DNA binding and activator recruitment activities of the NF-κB proteins.

The results also showed that NPM1 regulates specific NF-κB target genes by promoting the binding of NF-κB to those gene promoters. This specificity is at least dependent on the DNA sequences on the gene promoters. Because *in vitro* experiments showed that, NPM1 enhanced the binding of p65 to the specific DNA, although NF-κB p65 alone did not have the preference for binding to the κB containing DNA derived from different target gene promoters.

It is possible that the interaction of NPM1 may induce the conformational changes of p65 resulting in the sequence specificity of p65. Another possibility is that other NF-κB cofactor(s) might be involved in the regulation of these genes either by competing with NPM1 to bind to NF-κB or by compensating the function of NPM1 in NPM1 knockdown cells. For example, it has been reported that RPS3 interacts with p65 and regulates a subset of NF-κB target genes (22), cyclin-dependent kinase 6 interacts with p65 and is recruited to distinct chromatin regions of inflammatory genes (25), and telomerase binds to a subset of inflammatory gene promoters containing the T_2G_3 sequences and is required for efficient recruitment of p65 to these genes (24). It will be important to understand how these cofactors, including NPM1, cooperatively or independently regulate the NF-κB functions in inflammatory responses and cancer progression.

NF-κB mediated transcription does not simply depend on the amount of NF-κB. The posttranslational modifications and co-factors, as well as the chromatin structure around their target genes contribute to determining the NF-κB activity. Precisely controlled NF-κB activity is required for normal cell growth and immune and inflammatory responses (47). NPM1 is broadly expressed in normal cells and is suggested to contribute to the maintenance of appropriate NF-κB activity as it was shown to regulate NF-κB mediated transcription in fibroblasts and macrophages which are the components of tumor microenvironment (Fig. 8C and 8D). In addition, NPM1 may potentially contribute to the oncogenic NF-κB functions in cancer cells as it regulates the NF-κB mediated transcription in cancer cells (Fig. 2) and its expression level is correlated to NF-κB activity in colon adenoma and breast cancer cell lines (Fig. 8). The results that NPM1 regulated NF-κB mediated inflammatory genes in both cancer cells and normal cells like macrophages suggest the oncogenic role of NPM1 in both tumor cells and the tumor microenvironment through the regulation of NF-κB. Considering that NPM1 also shows other oncogenic

functions independent of NF-κB, such as regulating the activity and stability of p53 and ARF, cell growth, proliferation, and anti-apoptosis, it is likely that the expression level of NPM1 is a suitable diagnostic marker to determine the aggressiveness of cancer cells and also a suitable target of cancer therapy.

1-6. Figures and legends

Figure 1

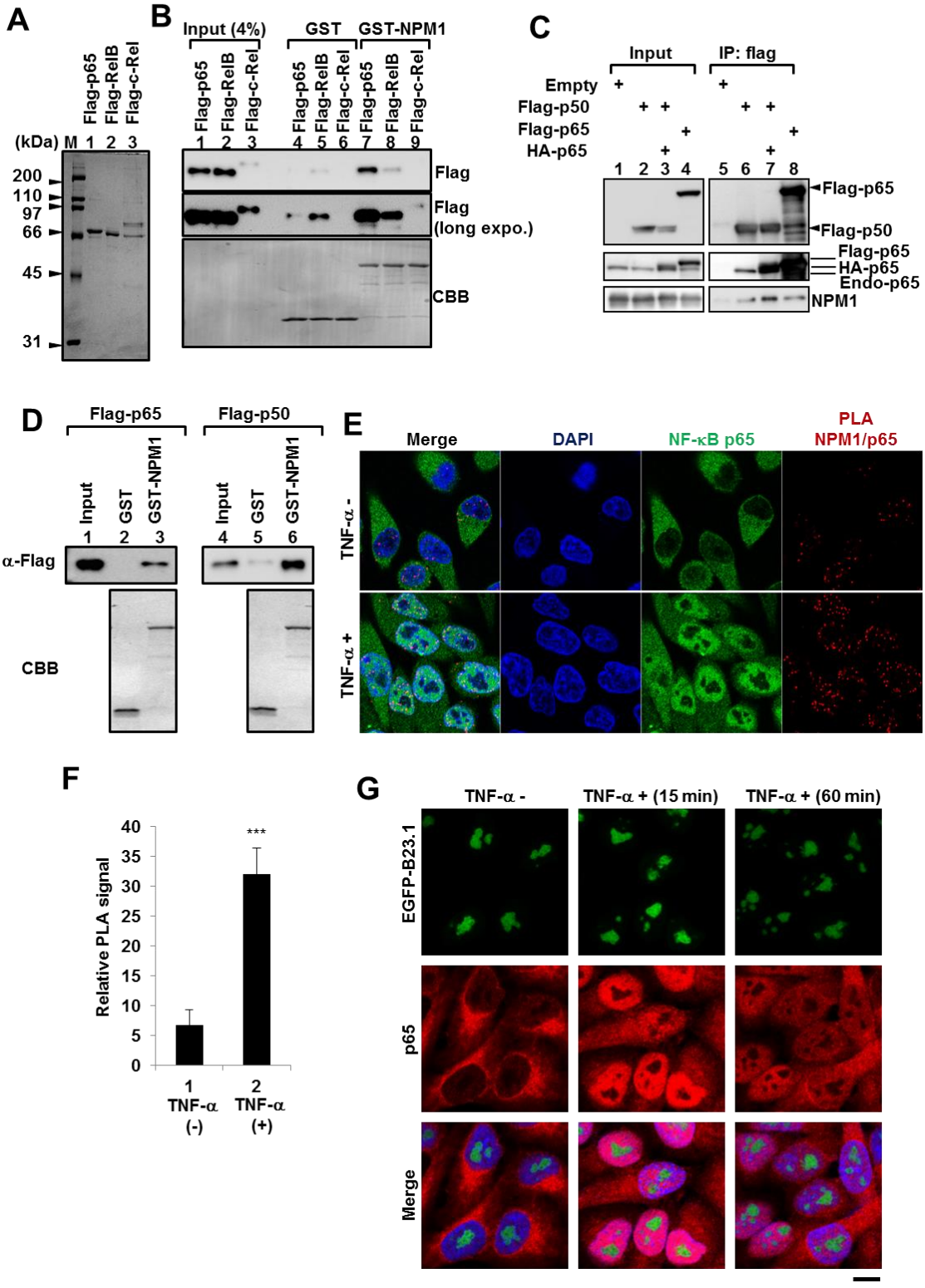

Fig. 1 Interaction between NPM1 and NF-κB

(A) Purified NF-κB proteins. Flag tagged p65, RelB, and c-Rel were expressed and purified with Flag-affinity gel, and the proteins were separated by 10% SDS-PAGE and visualized by CBB staining. (B) GST-pull down assays. GST pull-down assays using GST (lanes 4–6) or GST-NPM1 (lanes 7–9) with purified Flag-p65 (RelA), Flag-RelB, or c-Rel were performed. Flag-tagged NF-κB proteins were detected by western blotting and the GST proteins were visualized by CBB staining. (C) Immunoprecipitation assays. Flag-p65, Flag-p50, or Flag-p50/HA-p65 was expressed and the association with NPM1 was analyzed by immunoprecipitation (IP) with anti-Flag antibody followed by western blotting. (D) Flag-tagged p65 (lanes 1–3) and p50 (lanes 4–6) was mixed with GST or GST-NPM1 and the bound proteins with the GST proteins were examined by western blotting with anti-Flag antibody. The membranes for western blotting were stained with CBB to visualize the GST proteins. (E, F) *In vivo* interaction between NPM1 and p65. The interaction between NPM1 and p65 was examined by *in situ* proximity ligation assays (PLAs). HeLa cells were treated with or without 20 ng/ml TNF-α for 1 h, PLAs were performed using primary antibodies against NPM1 and p65. The PLA signals in panel C were quantitatively analyzed by the image processing software Imaris. The average spot number per cell was calculated from randomly selected cells (n=20). Error bars represent ±SD, statistical significance was calculated using student's *t*-test, and *** indicates $p<0.001$. (F) Localization of NPM1 in TNF-α treated cells. HeLa cells stably expressing EGFP-NPM1 were treated without or with TNF-α (20 ng/ml) for 15 min and 60 min, followed by immunofluorescence analysis with anti-p65 antibody, and the localization of the proteins was observed by a confocal microscope. Bar at the bottom indicates 10 μm.

Figure 2

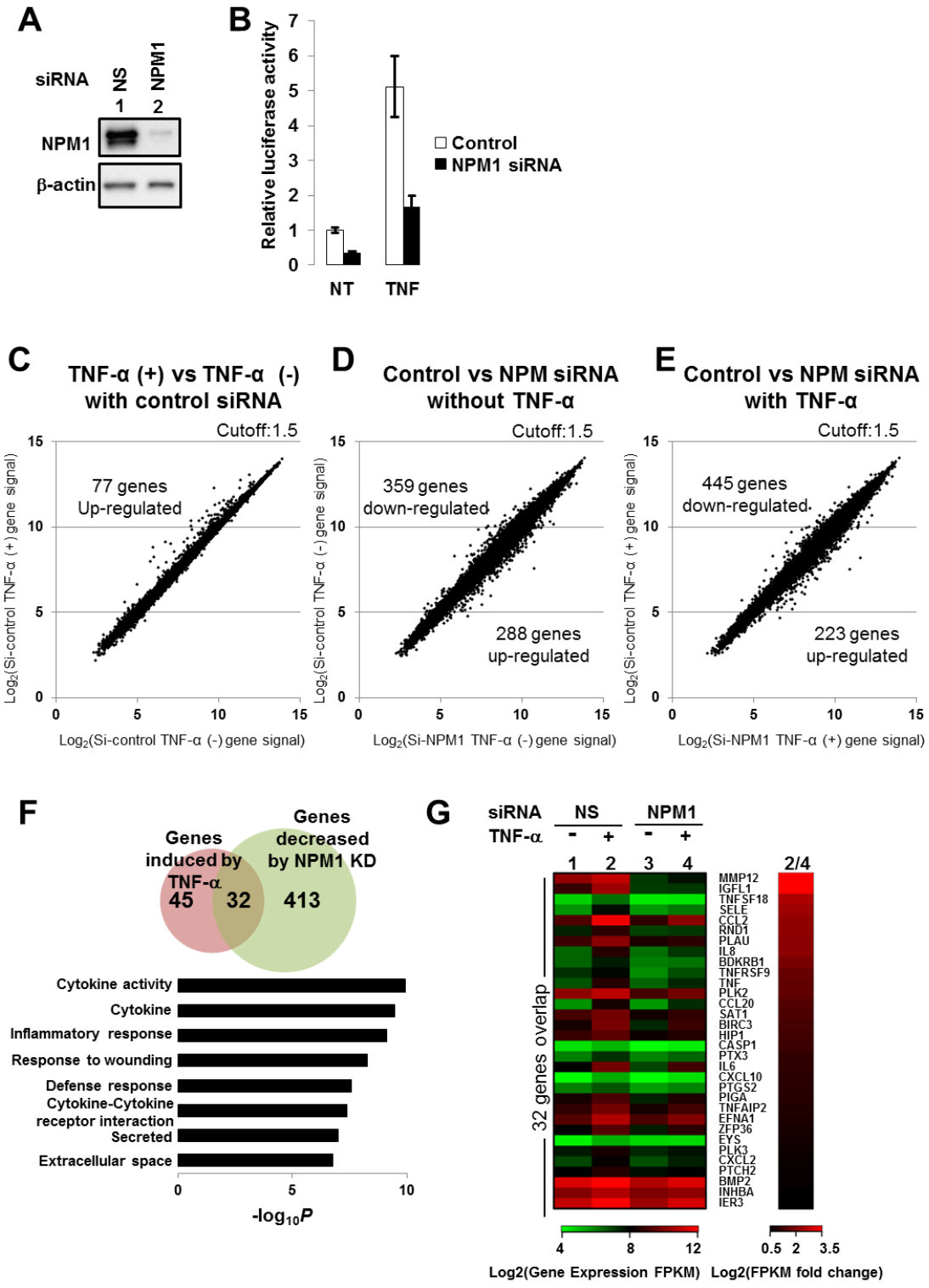
A
siRNA
NS
NPM1
1
2
NPM1
β-actin
B
Relative luciferase activity
Control
NPM1 siRNA
NT
TNF
C
TNF-α (+) vs TNF-α (-) with control siRNA
Cutoff:1.5
77 genes Up-regulated
Log2(Si-control TNF-α (+) gene signal)
Log2(Si-control TNF-α (-) gene signal)
D
Control vs NPM siRNA without TNF-α
Cutoff:1.5
359 genes down-regulated
288 genes up-regulated
Log2(Si-control TNF-α (-) gene signal)
Log2(Si-NPM1 TNF-α (-) gene signal)
E
Control vs NPM siRNA with TNF-α
Cutoff:1.5
445 genes down-regulated
223 genes up-regulated
Log2(Si-control TNF-α (+) gene signal)
Log2(Si-NPM1 TNF-α (+) gene signal)
F
Genes induced by TNF-α
Genes decreased by NPM1 KD
45
32
413
Cytokine activity
Cytokine
Inflammatory response
Response to wounding
Defense response
Cytokine-Cytokine receptor interaction
Secreted
Extracellular space
-log10P
G
siRNA
NS
NPM1
TNF-α
1
2
3
4
2/4
32 genes overlap
MMP12
IGFL1
TNFSF18
SELE
CCL2
RND1
PLAU
IL8
BDKRB1
TNFRSF9
TNF
PLK2
CCL20
SAT1
BIRC3
HIP1
CASP1
PTX3
IL6
CXCL10
PTGS2
PIGA
TNFAIP2
EFNA1
ZFP36
EYS
PLK3
CXCL2
PTCH2
BMP2
INHBA
IER3
Log2(Gene Expression FPKM)
Log2(FPKM fold change)

H

32 genes overlap (Figure 2C)

Gene	siCont/siNPM1	TNFα(+)/TNFα (-)
MMP12	10.89	1.72
IGFL1	10.64	3.12
TNFSF18	3.93	3.00
SELE	3.39	4.62
CCL2	3.07	5.85
RND1	3.05	2.38
PLAU	2.97	2.43
IL8	2.95	5.03
BDKRB1	2.61	2.21
TNFRSF9	2.34	1.64
TNF	2.28	3.81
PLK2	2.27	1.68
CCL20	2.09	7.06
SAT1	2.04	1.68
BIRC3	1.97	2.90
HIP1	1.93	1.57
CASP1	1.91	1.61
PTX3	1.80	2.46
IL6	1.78	3.95
CXCL10	1.76	2.53
PTGS2	1.74	1.66
PIGA	1.74	1.82
TNFAIP2	1.70	2.03
EFNA1	1.67	2.85
ZFP36	1.64	2.74
EYS	1.61	2.17
PLK3	1.59	1.67
CXCL2	1.58	2.38
PTCH2	1.56	1.54
BMP2	1.56	1.56
INHBA	1.53	1.73
IER3	1.52	1.92

I

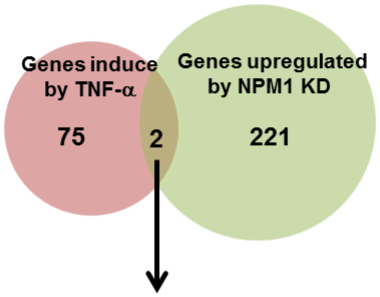

Gene	siNPM1/siCont	TNFα(+)/TNFα (-)
LYPD3	2.72	1.73
TAS2R20	1.74	1.54

J

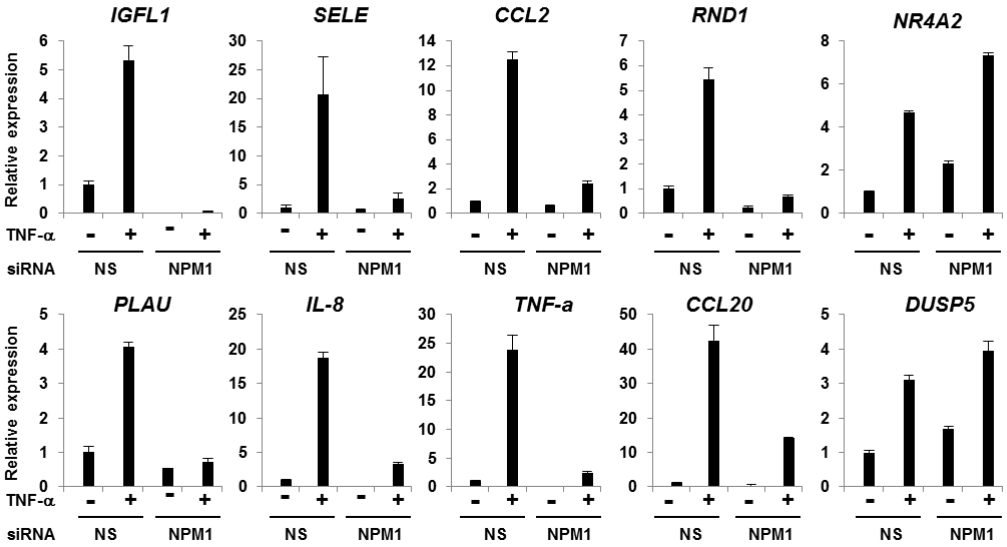

Fig. 2. NPM1 regulates NF-κB-dependent gene transcription

(A) Knockdown of NPM1 in HeLa cells by siRNA treatment. Western blotting confirmed the knockdown of NPM1 in HeLa cells. β-actin is a loading control. (B) Reporter assay. HeLa cells treated with NS or NPM1 siRNAs were transfected with p-κB-Luc and p-TA-RL plasmids. The cells were then stimulated without or with TNF-α for 3 h and subjected to luciferase assay. The

relative luciferase activity (fold increase) is shown. Three independent experiments were performed and error bars indicate ±SD. (C) Scatter plots of genes in HeLa cells treated with or without TNF-α (chip 1 vs chip 2). (D) Scatter plots of genes in HeLa cells transfected with control or NPM1 siRNA without TNF-α treatment (chip 1 vs chip 3). (E) Scatter plots of genes in HeLa cells transfected with control or NPM1 siRNA with TNF-α treatment (chip 2 vs chip 4). (F-I) Microarray analyses. RNAs were extracted from HeLa cells treated with control siRNA (chip 1 and 2) or NPM1 siRNA (chip 3 and 4) followed by stimulation without (chip1 and 3) or with TNF-α (chip 2 and 4), and subjected to microarray analyses. (F) The Venn diagram (upper panel) shows the coding genes induced by TNF-α treatment (chip 1 vs 2), the coding genes down-regulated by NPM1 knockdown in cells treated with TNF-α (chip 2 vs 4), and their overlapped genes. The overlapped 32 genes were subjected to gene ontology analysis and the list of the enriched functions is shown. Heat maps (G) depict the expression of the 32 overlapped genes (left) and the fold changes (right) between control and NPM1 knockdown cells treated with TNF-α (chip 2 vs 4). (H) The list of 32 genes shown in Figure 2D and fold changes of their expression level. (I) The Venn diagram shows the coding genes induced by TNF-α treatment (chip 1 vs 2), the coding genes up-regulated by NPM1 knockdown in cells treated with TNF-α (chip 2 vs 4), and their overlapped genes. The seven overlapped genes are shown.

(J) Confirmation of the microarray data by real-time RT-PCR analyses. RT-PCR for the genes involved in the list of (D) was performed using RNA extracted from cells treated with or without siRNAs and TNF-α as indicated at the bottom. RT-PCR was also examined for the two genes (*NR4A2* and *DUSP5*) that were up-regulated by NPM1 knockdown.

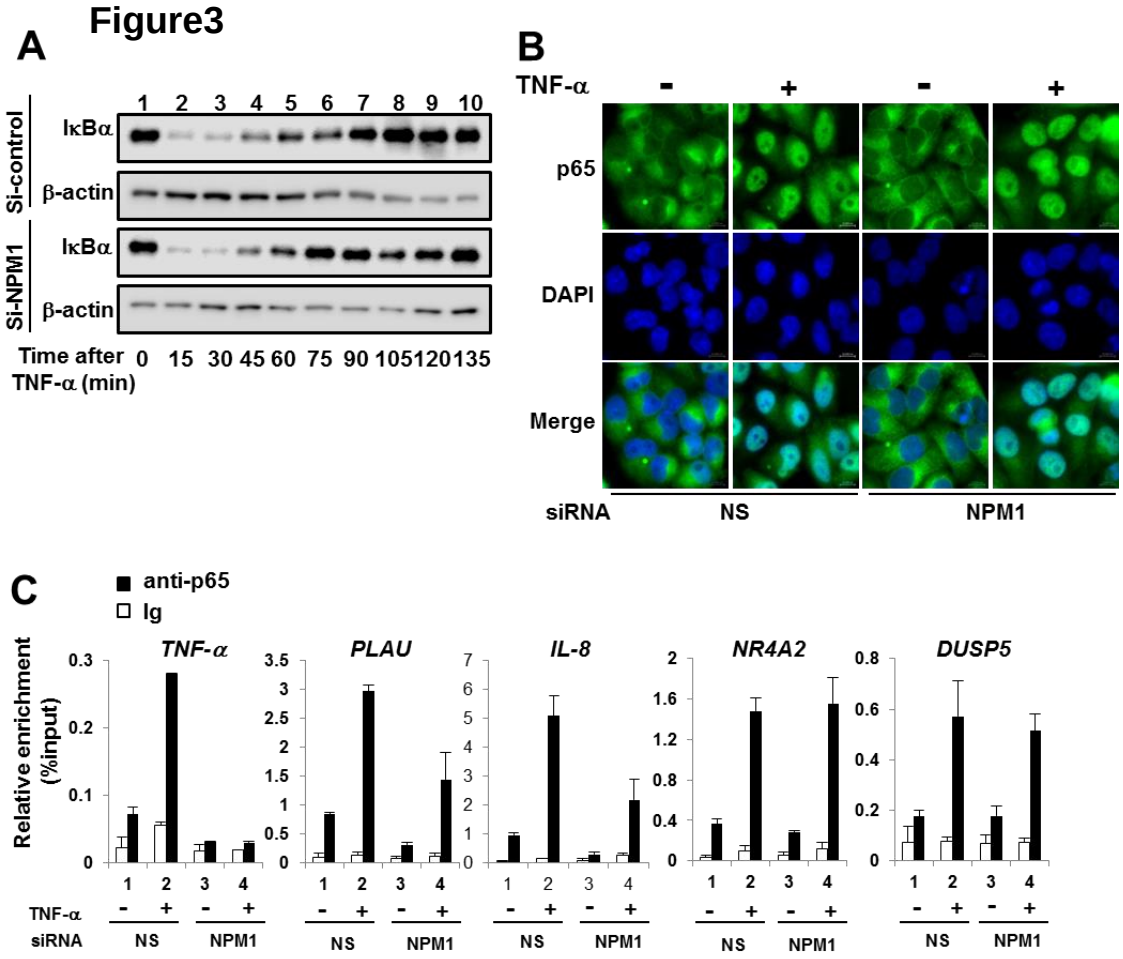

Fig. 3. NPM1 regulates the target gene binding of NF-κB, but not its nuclear translocation

(A) Effect of NPM1 knockdown on the expression level of I-κBα. The amounts of I-κBα and β-actin in HeLa cells treated with control siRNA or NPM1 siRNA after TNF-α treatment were examined by western blotting. Time (min) after TNF-α treatment is shown at the bottom of the panel. (B) Localization of p65 after TNF-α treatment in HeLa cells treated with control or NPM1 siRNA. DNA was counter stained by DAPI. (C) Recruitment of p65 to its target genes. HeLa cells transfected with siRNAs as indicated were incubated without or with TNF-α for 1 h, followed by ChIP assay. The precipitated DNA amounts containing the promoter regions of the genes listed in Fig. 2D (*TNF-α*, *PLAU*, and *IL-8*) and those of stimulated genes (*NR4A2* and *DUSP5*) by NPM1 knockdown were quantitatively analyzed by q-PCR. Three independent experiments were performed and error bars indicates ±SD.

Figure 4

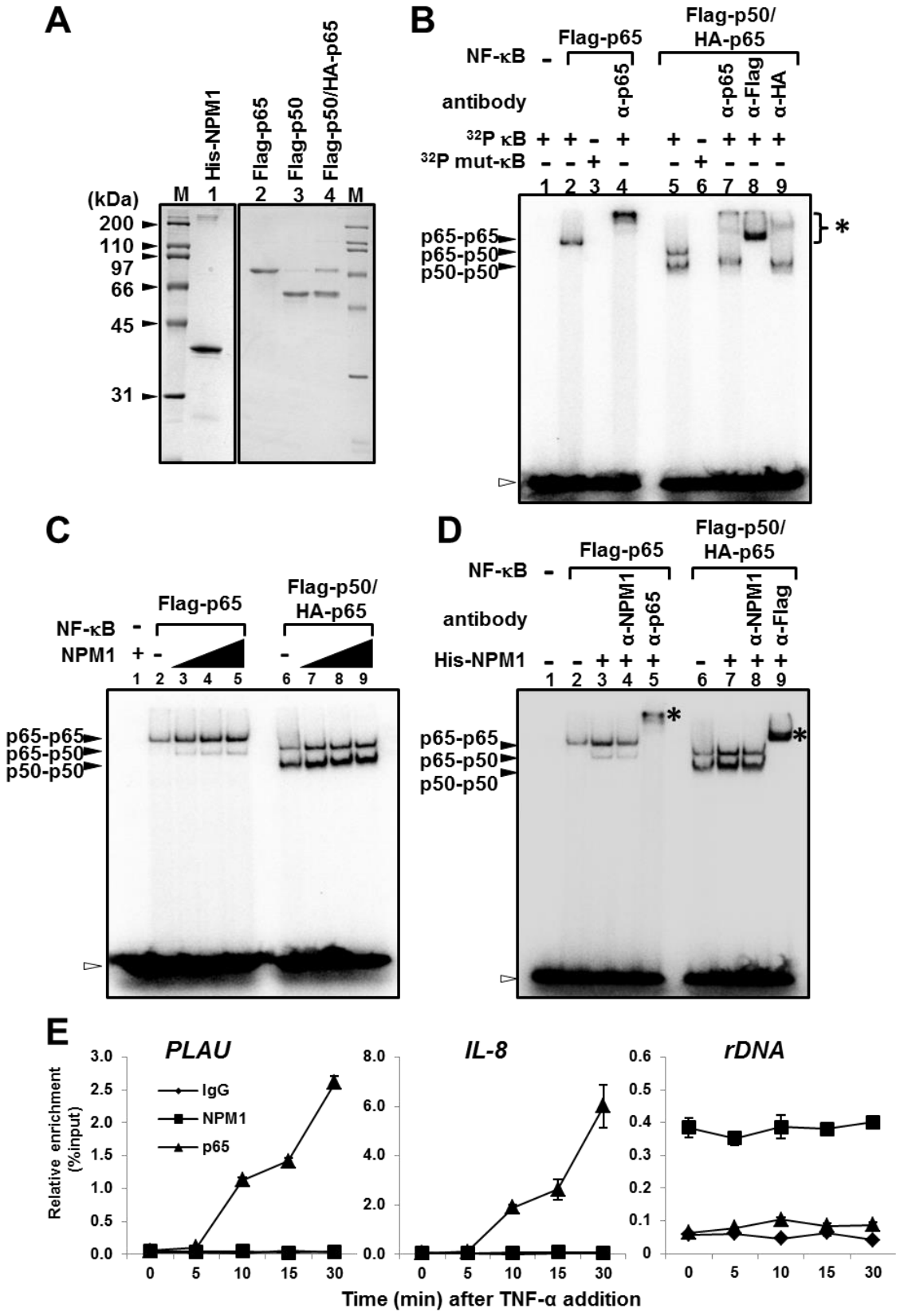
A
His-NPM1
Flag-p65
Flag-p50
Flag-p50/HA-p65
(kDa)
M 1 2 3 4 M
200
110
97
66
45
31
B
Flag-p65
Flag-p50/
HA-p65
NF-κB
antibody
α-p65
α-p65
α-Flag
α-HA
32P κB
32P mut-κB
1 2 3 4 5 6 7 8 9
p65-p65
p65-p50
p50-p50
*
C
Flag-p65
Flag-p50/
HA-p65
NF-κB
NPM1
1 2 3 4 5 6 7 8 9
p65-p65
p65-p50
p50-p50
D
Flag-p65
Flag-p50/
HA-p65
NF-κB
antibody
α-NPM1
α-p65
α-NPM1
α-Flag
His-NPM1
1 2 3 4 5 6 7 8 9
p65-p65
p65-p50
p50-p50
*
E
PLAU
IL-8
rDNA
IgG
NPM1
p65
Relative enrichment (%input)
Time (min) after TNF-α addition

Fig. 4. NPM1 enhances the DNA binding activity of NF-κB

(A) Purified proteins. His-tagged NPM1 and the NF-κB proteins purified with Flag-tag antibody were separated by SDS-PAGE and visualized by CBB staining. (B) EMSA with purified proteins. Purified recombinant NF-κB proteins (20 ng/sample) were analyzed by EMSA with a [^{32}P]-labeled, double-stranded wild-type (WT) or mutant (mut) κB oligonucleotides (300 fmole/sample). Antibodies against p65, Flag-tag, or HA-tag were added in the mixture as shown in lanes 4 and 7–9. (C) Effect of NPM1 on the DNA binding activity of the NF-κB proteins. Flag-p65 and Flag-p50/HA-p65 (20 ng, lane 2–5 and 6–9, respectively) were incubated with increasing amounts of His-NPM1 (0, 50, 100, and 200 ng), followed by EMSA with [^{32}P]-labeled probe (200 fmole/sample). The NPM1 alone (200 ng) were also incubated with the same probe (lane 1). (D) Supershift analysis with NPM1 antibody. Flag-p65 and Flag-p50/HA-p65 (20 ng, lanes 2–5 and 6–9, respectively) were incubated without or with His-NPM1 (200 ng) and indicated antibodies, followed by EMSA. The DNA bands bound by the p65–p65, p65–p50 and p50–p50 complexes, free probes, and supershifted bands are indicated by filled arrowheads, blank arrowheads, and asterisks, respectively (B–D). (E) Chromatin immunoprecipitation assay. HeLa cells were treated with TNF-α (20 ng/ml) for indicated time periods and then subjected to ChIP assays with control Ig, ant-p65, and anti-NPM1 antibodies. The *ribosomal RNA* gene coding region (*rDNA*) and the promoter regions of *PLAU* and *IL-8* genes were analyzed by qPCR.

Figure 5

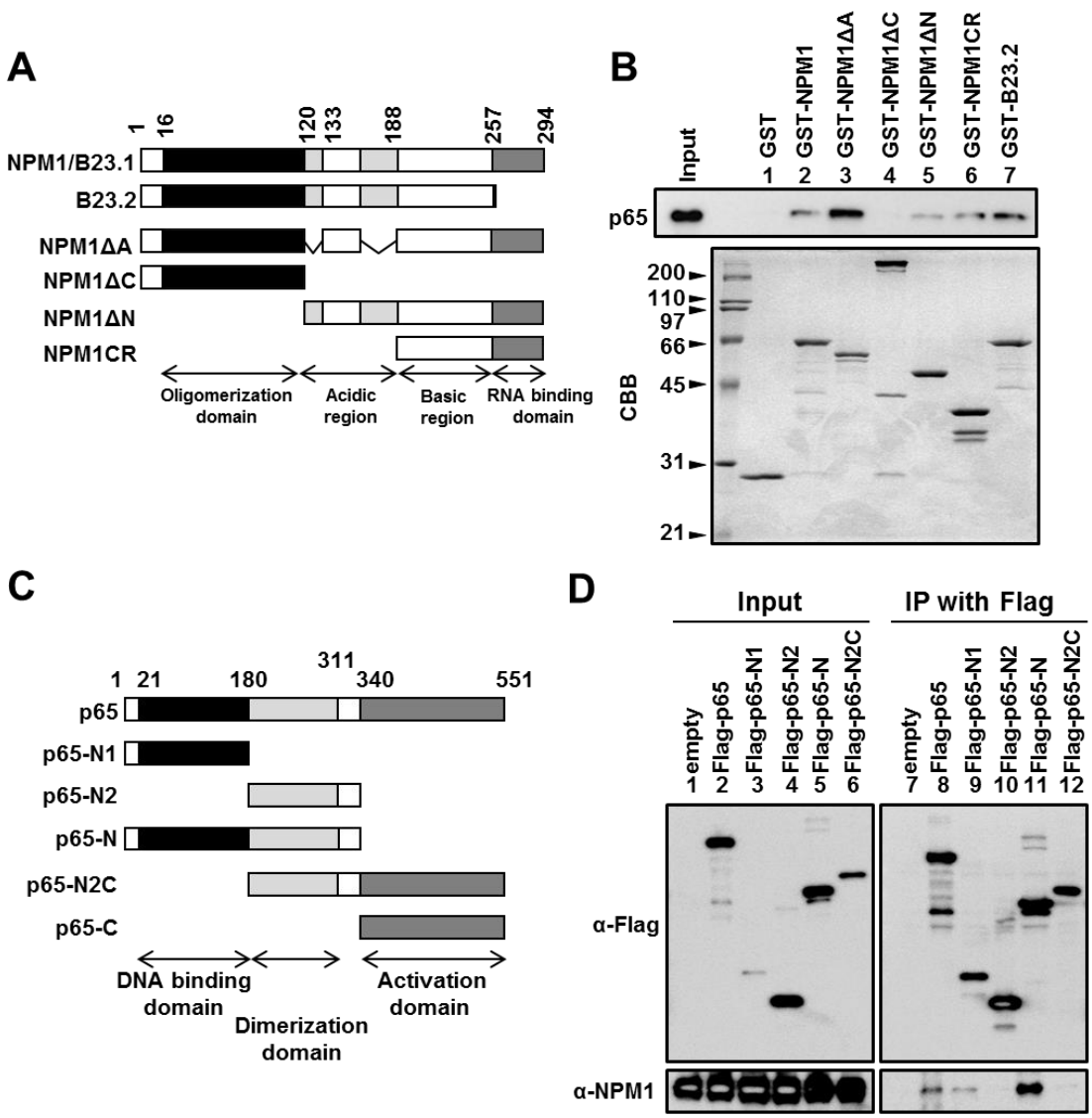

Fig. 5. The domain mapping of NPM1 and p65 required for their interaction

(A) Diagram of the splicing variants and truncation mutants of NPM1. Black boxes indicate oligomerization domain, light gray boxes at the central regions are acidic regions, dark gray indicates the C-terminal globular domain. (B) GST-pull down assay. GST or GST fusion proteins were incubated with purified Flag-p65 (500 ng/sample) and bound proteins were analyzed by SDS-PAGE,

followed by CBB staining for GST proteins (bottom panels) or western blotting with Flag antibody (top panels). (C) Diagram of the mutants of p65. The N-terminal DNA binding domain, dimerization domain, and the activation domain are shown by black, light gray, and dark gray boxes, respectively. (D) Immunoprecipitation analysis of the Flag-tagged p65 mutant proteins. Flag-tagged wild type and truncated p65 proteins were transiently expressed in 293T cells and immunoprecipitated with anti-Flag antibody. Input and immunoprecipitated proteins were analyzed by western blotting with anti-Flag and -NPM1 antibodies.

Figure 6

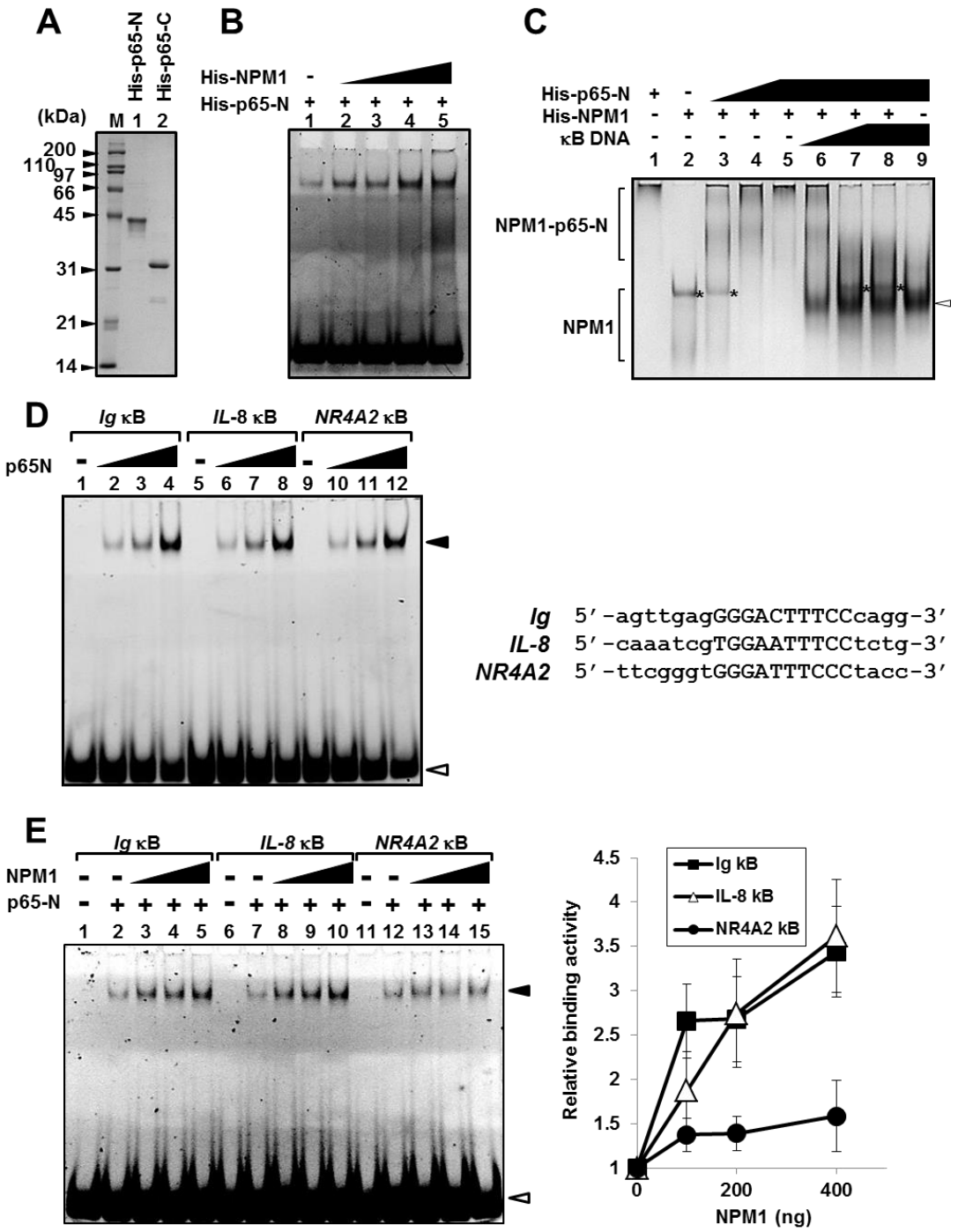

Fig. 6. The chaperone-like function of NPM1 enhances the binding of p65 to specific sequences

(A) Purified proteins. His-p65-N and His-p65-C were separated by SDS-PAGE and visualized by CBB staining. (B) Effect of NPM1 on the DNA binding activity

of p65-N. His-p65-N (40 ng, lane 1–5) were incubated with increasing amounts of His-NPM1 (0, 100, 200, 400 and 800 ng), and EMSA was performed. DNA was visualized by GelRed staining. (C) NPM1 and DNA complete for p65-N binding. His-NPM1 (60 pmole, lanes 2–8) was incubated with increasing amounts of His-p65-N (lanes 2–5, 0, 25, 50, 100 pmole, lanes 6–9, 100 pmole), then incubated without (lanes 1–5) or with increasing amounts of the κB DNA (for lanes 6–8, 40, 80, and 160 pmole, respectively). Lane 1 and 9 indicate His-p65-N alone (100 pmole) and the mixture of His-p65-N (100 pmole) and the κB DNA (160 pmole), respectively. The complexes were separated by native PAGE and visualized by CBB staining. Positions of free NPM1 are shown at the left side of the panel and the accumulated free NPM1 is also indicated by asterisks at the right side of the lanes. (D) The binding of p65-N to different DNA probes. Three κB DNA fragments (2 pmole) derived from *Ig*, *IL-8*, and *NR4A2* genes as shown at the right of the panel were incubated with increasing amounts of His-p65-N protein (0, 0.5, 1, 2 pmole, lanes 1-4, 5-8, 9-12, respectively), separated by native PAGE, and visualized by GelRed staining. The κB consensus sequences are indicated by capital letters. (E) NPM1 enhances the binding of p65-N to specific κB sites. The κB DNA fragments as in (D) were mixed with His-p65-N protein (0.5 pmole) pre-incubated with increasing amounts of His-NPM1 (0, 100, 200, 400, lanes 2-5, lanes 7-10, lanes 12-15), separated by native PAGE, and visualized by GelRed staining. Lanes 1, 6 and 11 indicate the kB DNA fragments without p65-N or NPM1. The intensity of the bands for p65-N-DNA complex were quantitatively analyzed and shown at the right graph. The experiments were repeated 5 times and error bars indicate ±SD. Blank and filled arrowheads in D and E show free DNA probes and the p65-N-DNA complexes, respectively.

Figure 7

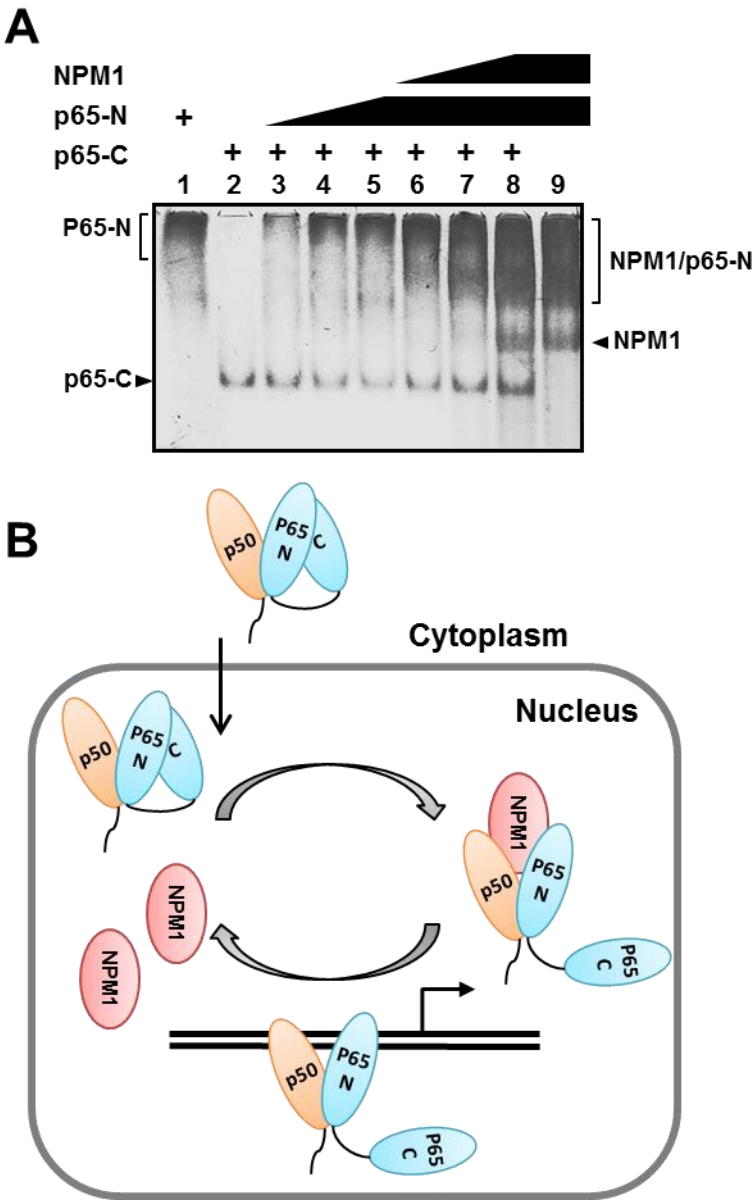

Fig. 7. NPM1 abrogates the intramolecular interaction of p65

(A) NPM1 abrogates the interaction between p65-N and p65-C. His-p65-C (lanes 2–8, 12 pmole) was incubated with increasing amounts of His-p65-N (lanes 2–5, 0, 9, 27, 54 pmole, and lanes 6–8, 54 pmole) and His-NPM1 (lanes 2–5, 0 pmol, lanes 6–8, 20, 40, 80 pmole), lane 1 indicates 54 pmole of His-p65-N alone, lane 9 indicates 80 pmole of His-NPM1 incubated with 54

pmole of His-p65-N. Proteins were separated by native PAGE and visualized by silver staining. (B) A working model of NF-κB-mediated transcription regulated by NPM1. Upon stimulation, the NF-κB is translocated to the nucleus where it associates with NPM1. The association of NPM1 enhances the DNA binding activity of NF-κB and abrogates the intramolecular interaction of p65. NPM1 releases NF-κB upon its binding to target DNA.

Figure 8

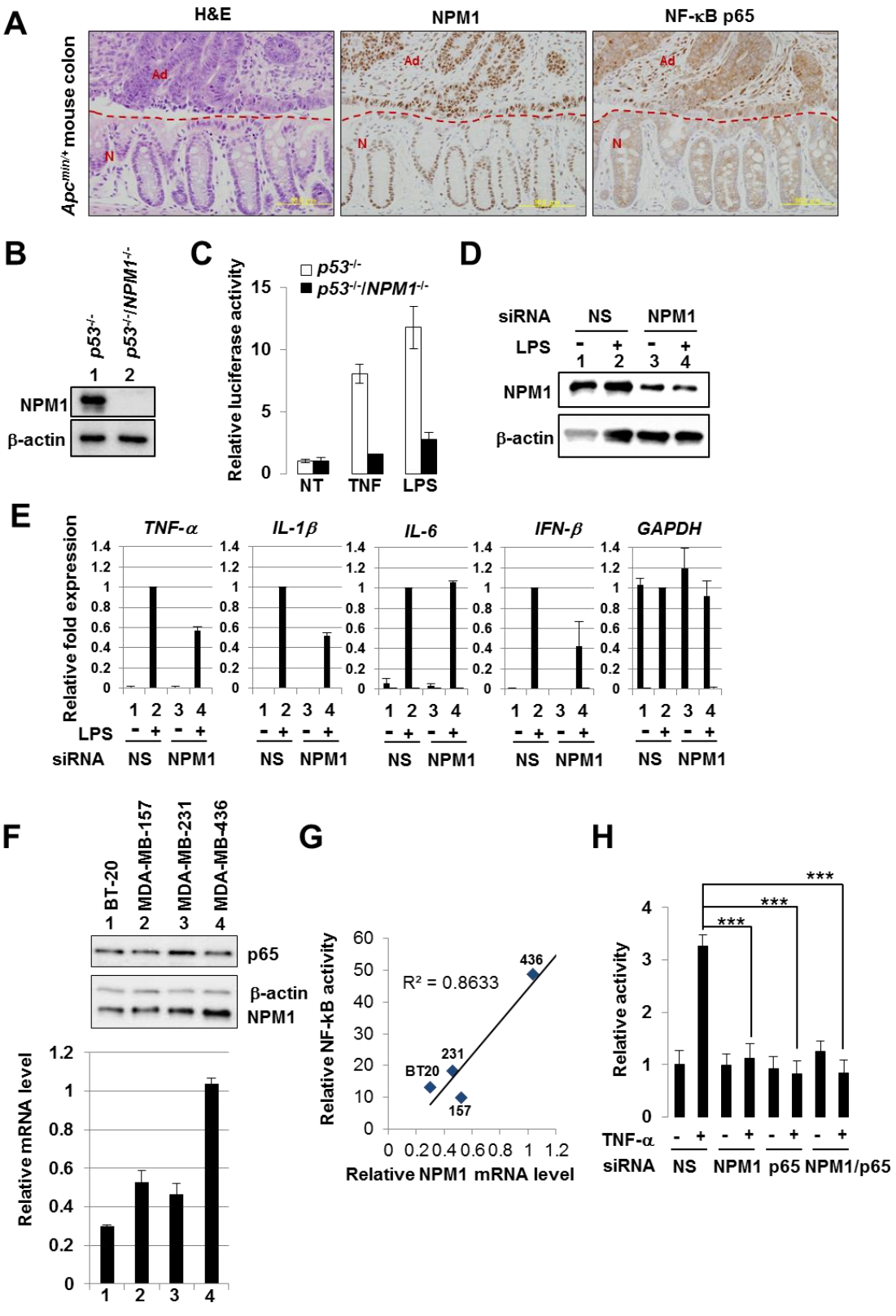
A
H&E
NPM1
NF-κB p65
Apc^min/+ mouse colon
Ad
N
B
p53-/-
p53-/-/NPM1-/-
NPM1
β-actin
C
p53-/-
p53-/-/NPM1-/-
Relative luciferase activity
NT
TNF
LPS
D
siRNA
NS
NPM1
LPS
NPM1
β-actin
E
TNF-α
IL-1β
IL-6
IFN-β
GAPDH
Relative fold expression
LPS
siRNA
NS
NPM1
F
BT-20
MDA-MB-157
MDA-MB-231
MDA-MB-436
p65
β-actin
NPM1
Relative mRNA level
G
Relative NF-kB activity
R² = 0.8633
436
231
BT20
157
Relative NPM1 mRNA level
H
Relative activity
TNF-α
siRNA
NS
NPM1
p65
NPM1/p65

Fig. 8. Functional intersection between NPM1 and NF-κB signaling

(A) Expression and localization of NPM1 and p65 in inflammatory colon in *Apc*$^{min/+}$ mice. Hematoxylin and eosin (HE) staining, and immunohistochemistry with anti-NPM1 and anti-p65 antibodies are shown as indicated. “N” and “Ad” represent normal and adenoma, respectively. Scale bars indicate 50 μm. (B) Western blotting of *p53*$^{-/-}$ and *p53*$^{-/-}$*NPM1*$^{-/-}$ MEFs with anti-NPM1 and anti-β actin. (C) The NF-κB-dependent reporter activity in MEFs. *p53*$^{-/-}$ and *p53*$^{-/-}$*NPM1*$^{-/-}$ MEFs transfected with reporter plasmids for 16 h, stimulated without or with TNF-α (20 ng/ml) or LPS (1 μg/ml) for 3 h, and examined for luciferase activity. The relative NF-κB-driven luciferase activity (fold increase) is shown. Three independent experiments were performed and error bars are ± SD. (D) Western blotting of mouse peritoneal macrophages. Mouse peritoneal macrophages were transfected with NS or NPM1 siRNA for 72 h, followed by treatment with or without LPS (1 μg/ml) for 2 h. The extracts were subjected to western blotting with anti-NPM1 and anti-β actin antibodies. (E) Expression of cytokine genes in macrophages. Total RNAs were extracted from cells as in (D) and the expressions of cytokines (*TNF-α, IL-1β*, *IL-6*, *IFN-β*) and *GAPDH* were analyzed by RT-qPCR. (F) Expression of NPM1 in breast cancer cell lines. Cell extracts (2 and 4 μg of proteins for top and middle panels, respectively) from BT-20, MDA-MB-157, MDA-MB-231, or MDA-MB-436 cells were separated by 10% SDS-PAGE and the expression of p65, β-actin, and NPM1 was examined by western blotting (top and middle panels). Total RNA was extracted from the cells and the expression of NPM1 and β-actin mRNA was quantitatively analyzed. The amount of NPM1 mRNA was normalized by that of β-actin and shown in bottom graph. (G) Relationship between the NF-κB activity and NPM1 expression level. The constitutive NF-κB activity obtained from previously published data (42) was plotted as a function of the NPM1 mRNA level shown in (F). (H) Invasion activity of MDA-MB-231 cells. MDA-MB-231 cells were transfected with NS, NPM1, p65, or NPM1 and p65

siRNAs for 48 h, seeded in transwells coated with Matrigel, and treated without or with TNF-*α* for 16 h. Representative images of the bottom surface are shown in Fig. S5B. Cell number detected at the bottom surface of control siRNA-treated and non-stimulated cells was set as 1.0, and relative cell numbers were quantitatively analyzed. Cell numbers were averages of 4 random microscopic fields from 3 independent experiments. *** indicates $p < 0.001$.

Fig. 9

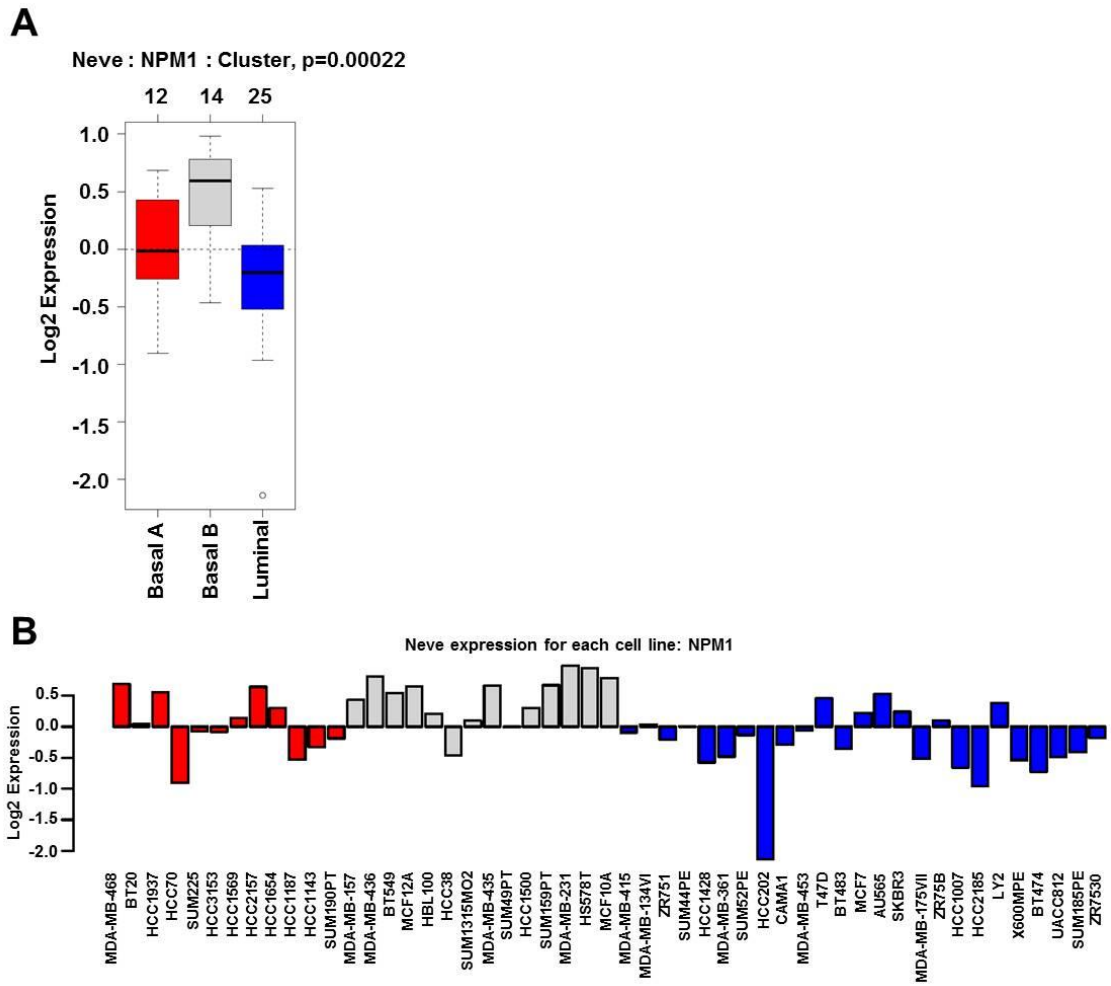

Fig. 9. Expression of NPM1 in breast cancer cell lines

Expression of NPM1 in commonly used 51 breast cancer cell lines were examined by the GOBO database (http://co.bmc.lu.se/gobo/gsa.pl). Average

NPM1 expression in 12 Basal A (red), 14 Basal B (gray), and 25 Luminal (blue) cell lines are indicated as box plot (A) and the NPM1 expression in individual cells are shown in (B).

Fig. 10

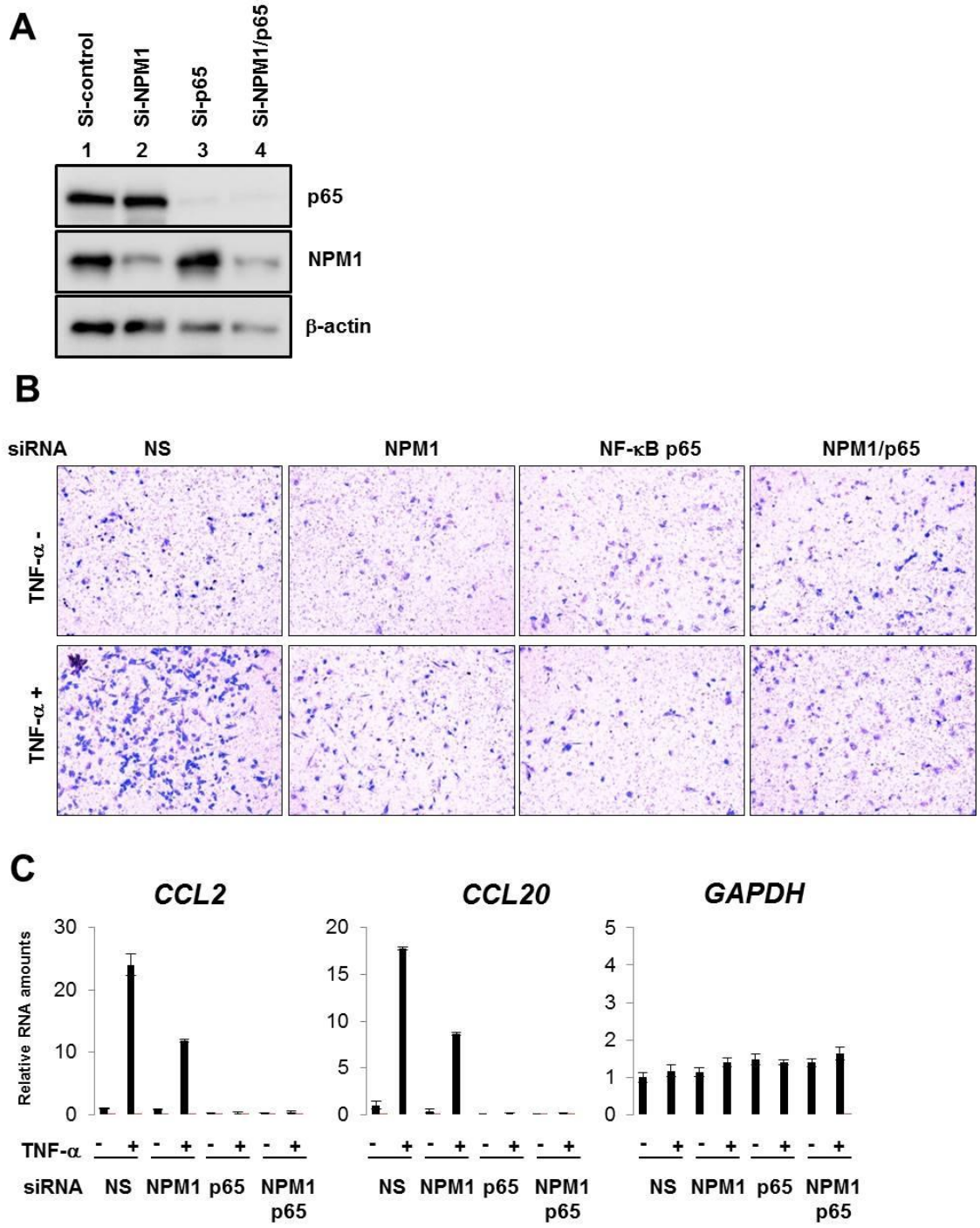

Fig. 10. NF-kB mediated invasion activity of MDA-MB-231 cells regulated by NPM1

(A) Western blotting. MDA-MB-231 cells were transfected with siRNAs as indicated at the top of the gel and the expression level of proteins was analyzed by western blotting. (B) Invasion activity of MDA-MB-231 cells.

MDA-MB-231 cells were transfected with NS, NPM1, p65, or NPM1 and p65 siRNAs for 48 h, seeded in transwells coated with Matrigel, and treated without or with TNF-*α* for 16 h. Representative images of the bottom surface are shown. (C) RT-qPCR. The cells prepared as in (A) were treated without or with TNF-α for 12 hrs, and RNAs were extracted from cells prepared as in A and analyzed by RT-qPCR. The experiments were independently repeated three times and error bars indicate ±SD.

1-7. Table for primers

Table 1. Primer sets for RT-PCR

NR4A2 F	GTATGGGTCCTCGCCTCAAG
NR4A2 R	AGCCTGTGCTGTAGTTGTCC
DUSP5 F	ACAGCCCTGCTGAATGTCTC
DUSP5 R	GGAGCTAATGTCAGCCGTGT
CCL20 F	GAATCAGAAGCAGCAAGCAAC
CCL20 R	TTGCGCACACAGACAACTTTTT
CCL2 F	GATCTCAGTGCAGAGGCTCG
CCL2 R	TTTGCTTGTCCAGGTGGTCC
PLAU F	GACTCCAAAGGCAGCAATGA
PLAU R	TGCTGCCCTCCGAATTTCTT
SELE F	CCGAGCGAGGCTACATGAAT
SELE R	GCCACATTGGAGCCTTTTGG
RND1 F	CAGCGACTCGGATGCAGTAT
RND1 R	CTGTCTTGCAGCCAATGAGC
IL-8 F	TAGCAAAATTGAGGCCAAGG
IL-8 R	AAACCAAGGCACAGTGGAAC
TNF-a F	TCCTTCAGACACCCTCAACC
TNF-a R	AGGCCCCAGTTTGAATTCTT
IkBa F	CTCCGAGACTTTCGAGGAAATAC
IkBa R	GCCATTGTAGTTGGTAGCCTTCA
GAPDH F	CCACATCGCTCAGACACCAT
GAPDH R	GCGCCCAATACGACCAAA
hCXCR4 F	TCCATTCCTTTGCCTCTTTTGC
hCXCR4 R	ACGGAAACAGGGTTCCTTCAT
Mouse TNF-a F	ACA AGGCTGCCCCGACTA C
Mouse TNF-a R	TGGAAGACTCCTCCCAGGTATATG
Mouse IL-6 F	CCCAATTTCCAATGCTCTCC
Mouse IL-6 R	TCCACAAACTGATATGCTTAGG
Mouse IFN-β-F	CAGCTCCAAGAAAGGACGAAC
Mouse IFN-β-R	GGCAGTGTAACTCTTCTGCAT
Mouse IL-1 β F	CTTCAAATCTCACAGCAGCACATC
Mouse IL-1 β R	CCACGGGAAAGACACAGGTAG
Mouse CCL2 F	CCCCACTCACCTGCTGCTAC
Mouse CCL2 R	CCTGCTGCTGGTGATTCTCTT
Mouse GADPH F	ACCCAGAAGACTGTGGATGG
Mouse GADPH R	CACATTGGGGGTAGGAACAC

Table 2. Primer sequences for ChIP-PCR assays

DUSP5 F	CTTATATGGGCAGCCGCGT
DUSP5 R	CTAGAAGCCGGGGATTCCG
NR4A2 F	CTCTGAGCGTCTCGTGTCATG
NR4A2 R	CCCCCTTAGCGGAAGAGC
IL-8 F	ATCAGTTGCAAATCGTGGA
IL-8 R	TGCCTTATGGAGTGCTCCGGTG
TNF-a F	CCACAGCAATGGGTAGGAGAATG
TNF-a R	TTCATGAAGCTCTCACTTCTCAG
PLAU F	AGCAATCAGCATGACAGCCT
PLAU R	CTGCAGCCTGAGGACTTACC
rDNA #3 F	CTCTTAGCGGTGGATCACTCG
rDNA#3 R	GCTAGCTGCGTTCTTCATCGA

1-8. References

1. Foulds, L. (1954) The Experimental Study of Tumor Progression - a Review. *Cancer Res*, **14**, 327-339.
2. Hanahan, D. and Weinberg, R.A. (2011) Hallmarks of cancer: the next generation. *Cell*, **144**, 646-674.
3. Tredan, O., Galmarini, C.M., Patel, K. and Tannock, I.F. (2007) Drug resistance and the solid tumor microenvironment. *J Natl Cancer Inst*, **99**, 1441-1454.
4. Wang, D.J., Ratnam, N.M., Byrd, J.C. and Guttridge, D.C. (2014) NF-kappaB functions in tumor initiation by suppressing the surveillance of both innate and adaptive immune cells. *Cell Rep*, **9**, 90-103.
5. Pikarsky, E., Porat, R.M., Stein, I., Abramovitch, R., Amit, S., Kasem, S., Gutkovich-Pyest, E., Urieli-Shoval, S., Galun, E. and Ben-Neriah, Y. (2004) NF-kappaB functions as a tumour promoter in inflammation-associated cancer. *Nature*, **431**, 461-466.
6. Luo, J.L., Maeda, S., Hsu, L.C., Yagita, H. and Karin, M. (2004) Inhibition of NF-kappaB in cancer cells converts inflammation- induced tumor growth mediated by TNFalpha to TRAIL-mediated tumor regression. *Cancer Cell*, **6**, 297-305.
7. Greten, F.R., Eckmann, L., Greten, T.F., Park, J.M., Li, Z.W., Egan, L.J., Kagnoff, M.F. and Karin, M. (2004) IKKbeta links inflammation and tumorigenesis in a mouse model of colitis-associated cancer. *Cell*, **118**, 285-296.
8. Sen, R. and Baltimore, D. (1986) Multiple nuclear factors interact with the immunoglobulin enhancer sequences. *Cell*, **46**, 705-716.
9. Gilmore, T.D. (2006) Introduction to NF-kappaB: players, pathways, perspectives. *Oncogene*, **25**, 6680-6684.
10. Hayden, M.S. and Ghosh, S. (2012) NF-kappaB, the first quarter-century: remarkable progress and outstanding questions. *Genes Dev*, **26**, 203-234.
11. Phelps, C.B., Sengchanthalangsy, L.L., Malek, S. and Ghosh, G. (2000) Mechanism of kappa B DNA binding by Rel/NF-kappa B dimers. *J Biol Chem*, **275**, 24392-24399.
12. Zabel, U., Schreck, R. and Baeuerle, P.A. (1991) DNA binding of purified transcription factor NF-kappa B. Affinity, specificity, Zn2+ dependence, and differential half-site recognition. *J Biol Chem*, **266**, 252-260.
13. Wan, F., Anderson, D.E., Barnitz, R.A., Snow, A., Bidere, N., Zheng, L., Hegde, V., Lam, L.T., Staudt, L.M., Levens, D. *et al.* (2007) Ribosomal protein S3: a KH domain subunit in NF-kappaB complexes that mediates selective gene regulation. *Cell*, **131**, 927-939.
14. Fu, K., Sun, X., Zheng, W., Wier, E.M., Hodgson, A., Tran, D.Q., Richard, S. and Wan, F. (2013) Sam68 modulates the promoter specificity of NF-kappaB and mediates expression of CD25 in activated T cells. *Nat Commun*, **4**, 1909.
15. Ghosh, A., Saginc, G., Leow, S.C., Khattar, E., Shin, E.M., Yan, T.D., Wong, M., Zhang, Z., Li, G., Sung, W.K. *et al.* (2012) Telomerase directly regulates NF-kappaB-dependent transcription. *Nat Cell Biol*, **14**, 1270-1281.
16. Handschick, K., Beuerlein, K., Jurida, L., Bartkuhn, M., Muller, H., Soelch, J.,

Weber, A., Dittrich-Breiholz, O., Schneider, H., Scharfe, M. *et al.* (2014) Cyclin-dependent kinase 6 is a chromatin-bound cofactor for NF-kappaB-dependent gene expression. *Mol Cell*, **53**, 193-208.

17. Dhar, S.K., Lynn, B.C., Daosukho, C. and St Clair, D.K. (2004) Identification of nucleophosmin as an NF-kappaB co-activator for the induction of the human SOD2 gene. *J Biol Chem*, **279**, 28209-28219.
18. Borer, R.A., Lehner, C.F., Eppenberger, H.M. and Nigg, E.A. (1989) Major nucleolar proteins shuttle between nucleus and cytoplasm. *Cell*, **56**, 379-390.
19. Okuwaki, M., Iwamatsu, A., Tsujimoto, M. and Nagata, K. (2001) Identification of nucleophosmin/B23, an acidic nucleolar protein, as a stimulatory factor for in vitro replication of adenovirus DNA complexed with viral basic core proteins. *J Mol Biol*, **311**, 41-55.
20. Murano, K., Okuwaki, M., Hisaoka, M. and Nagata, K. (2008) Transcription regulation of the rRNA gene by a multifunctional nucleolar protein, B23/nucleophosmin, through its histone chaperone activity. *Mol Cell Biol*, **28**, 3114-3126.
21. Savkur, R.S. and Olson, M.O. (1998) Preferential cleavage in pre-ribosomal RNA byprotein B23 endoribonuclease. *Nucleic Acids Res*, **26**, 4508-4515.
22. Okuwaki, M., Sumi, A., Hisaoka, M., Saotome-Nakamura, A., Akashi, S., Nishimura, Y. and Nagata, K. (2012) Function of homo- and hetero-oligomers of human nucleoplasmin/nucleophosmin family proteins NPM1, NPM2 and NPM3 during sperm chromatin remodeling. *Nucleic Acids Res*, **40**, 4861-4878.
23. Okuda, M., Horn, H.F., Tarapore, P., Tokuyama, Y., Smulian, A.G., Chan, P.K., Knudsen, E.S., Hofmann, I.A., Snyder, J.D., Bove, K.E. *et al.* (2000) Nucleophosmin/B23 is a target of CDK2/cyclin E in centrosome duplication. *Cell*, **103**, 127-140.
24. Koike, A., Nishikawa, H., Wu, W., Okada, Y., Venkitaraman, A.R. and Ohta, T. (2010) Recruitment of phosphorylated NPM1 to sites of DNA damage through RNF8-dependent ubiquitin conjugates. *Cancer Res*, **70**, 6746-6756.
25. Okuwaki, M., Matsumoto, K., Tsujimoto, M. and Nagata, K. (2001) Function of nucleophosmin/B23, a nucleolar acidic protein, as a histone chaperone. *Febs Lett*, **506**, 272-276.
26. Falini, B., Mecucci, C., Tiacci, E., Alcalay, M., Rosati, R., Pasqualucci, L., La Starza, R., Diverio, D., Colombo, E., Santucci, A. *et al.* (2005) Cytoplasmic nucleophosmin in acute myelogenous leukemia with a normal karyotype. *N Engl J Med*, **352**, 254-266.
27. Grisendi, S., Mecucci, C., Falini, B. and Pandolfi, P.P. (2006) Nucleophosmin and cancer. *Nat Rev Cancer*, **6**, 493-505.
28. Zeller, K.I., Haggerty, T.J., Barrett, J.F., Guo, Q., Wonsey, D.R. and Dang, C.V. (2001) Characterization of nucleophosmin (B23) as a Myc target by scanning chromatin immunoprecipitation. *J Biol Chem*, **276**, 48285-48291.
29. Tsui, K.H., Cheng, A.J., Chang, P., Pan, T.L. and Yung, B.Y. (2004) Association of nucleophosmin/B23 mRNA expression with clinical outcome in patients with bladder carcinoma. *Urology*, **64**, 839-844.

30. Hisaoka, M., Nagata, K. and Okuwaki, M. (2014) Intrinsically disordered regions of nucleophosmin/B23 regulate its RNA binding activity through their inter- and intra-molecular association. *Nucleic Acids Res*, **42**, 1180-1195.
31. Steffensen, I.L., Paulsen, J.E., Eide, T.J. and Alexander, J. (1997) 2-Amino-1-methyl-6-phenylimidazo[4,5-b]pyridine increases the numbers of tumors, cystic crypts and aberrant crypt foci in multiple intestinal neoplasia mice. *Carcinogenesis*, **18**, 1049-1054.
32. Hisaoka, M., Ueshima, S., Murano, K., Nagata, K. and Okuwaki, M. (2010) Regulation of nucleolar chromatin by B23/nucleophosmin jointly depends upon its RNA binding activity and transcription factor UBF. *Mol Cell Biol*, **30**, 4952-4964.
33. Hisaoka, M., Nagata, K. and Okuwaki, M. (2014) Intrinsically disordered regions of nucleophosmin/B23 regulate its RNA binding activity through their inter- and intra-molecular association. *Nucleic Acids Res*, **42**, 1180-1195.
34. Gentleman, R.C., Carey, V.J., Bates, D.M., Bolstad, B., Dettling, M., Dudoit, S., Ellis, B., Gautier, L., Ge, Y., Gentry, J. *et al.* (2004) Bioconductor: open software development for computational biology and bioinformatics. *Genome biology*, **5**, R80.
35. Gautier, L., Cope, L., Bolstad, B.M. and Irizarry, R.A. (2004) affy - analysis of Affymetrix GeneChip data at the probe level. *Bioinformatics*, **20**, 307-315.
36. Irizarry, R.A., Bolstad, B.M., Collin, F., Cope, L.M., Hobbs, B. and Speed, T.P. (2003) Summaries of Affymetrix GeneChip probe level data. *Nucleic Acids Res*, **31**, e15.
37. Irizarry, R.A., Hobbs, B., Collin, F., Beazer-Barclay, Y.D., Antonellis, K.J., Scherf, U. and Speed, T.P. (2003) Exploration, normalization, and summaries of high density oligonucleotide array probe level data. *Biostatistics*, **4**, 249-264.
38. Huang, D.W., Sherman, B.T., Tan, Q., Collins, J.R., Alvord, W.G., Roayaei, J., Stephens, R., Baseler, M.W., Lane, H.C. and Lempicki, R.A. (2007) The DAVID Gene Functional Classification Tool: a novel biological module-centric algorithm to functionally analyze large gene lists. *Genome Biol*, **8**, R183.
39. Huang, D.W., Sherman, B.T., Tan, Q., Kir, J., Liu, D., Bryant, D., Guo, Y., Stephens, R., Baseler, M.W., Lane, H.C. *et al.* (2007) DAVID Bioinformatics Resources: expanded annotation database and novel algorithms to better extract biology from large gene lists. *Nucleic Acids Res*, **35**, W169-175.
40. Sun, S.C., Ganchi, P.A., Ballard, D.W. and Greene, W.C. (1993) NF-kappa B controls expression of inhibitor I kappa B alpha: evidence for an inducible autoregulatory pathway. *Science*, **259**, 1912-1915.
41. Zhong, H., Voll, R.E. and Ghosh, S. (1998) Phosphorylation of NF-kappa B p65 by PKA stimulates transcriptional activity by promoting a novel bivalent interaction with the coactivator CBP/p300. *Mol Cell*, **1**, 661-671.
42. Karin, M. (2006) Nuclear factor-kappaB in cancer development and progression. *Nature*, **441**, 431-436.
43. Colombo, E., Bonetti, P., Lazzerini Denchi, E., Martinelli, P., Zamponi, R., Marine, J.C., Helin, K., Falini, B. and Pelicci, P.G. (2005) Nucleophosmin is required for DNA integrity and p19Arf protein stability. *Molecular and cellular biology*, **25**,

8874-8886.

44. Ringner, M., Fredlund, E., Hakkinen, J., Borg, A. and Staaf, J. (2011) GOBO: gene expression-based outcome for breast cancer online. *Plos One*, **6**, e17911.

45. Yamaguchi, N., Ito, T., Azuma, S., Ito, E., Honma, R., Yanagisawa, Y., Nishikawa, A., Kawamura, M., Imai, J., Watanabe, S. *et al.* (2009) Constitutive activation of nuclear factor-kappaB is preferentially involved in the proliferation of basal-like subtype breast cancer cell lines. *Cancer Sci*, **100**, 1668-1674.

46. Karhemo, P.R., Rivinoja, A., Lundin, J., Hyvonen, M., Chernenko, A., Lammi, J., Sihto, H., Lundin, M., Heikkila, P., Joensuu, H. *et al.* (2011) An extensive tumor array analysis supports tumor suppressive role for nucleophosmin in breast cancer. *Am J Pathol*, **179**, 1004-1014.

47. Neve, R.M., Chin, K., Fridlyand, J., Yeh, J., Baehner, F.L., Fevr, T., Clark, L., Bayani, N., Coppe, J.P., Tong, F. *et al.* (2006) A collection of breast cancer cell lines for the study of functionally distinct cancer subtypes. *Cancer Cell*, **10**, 515-527.

48. Fang, W.B., Jokar, I., Zou, A., Lambert, D., Dendukuri, P. and Cheng, N. (2012) CCL2/CCR2 chemokine signaling coordinates survival and motility of breast cancer cells through Smad3 protein- and p42/44 mitogen-activated protein kinase (MAPK)-dependent mechanisms. *J Biol Chem*, **287**, 36593-36608.

49. Marsigliante, S., Vetrugno, C. and Muscella, A. (2013) CCL20 induces migration and proliferation on breast epithelial cells. *J Cell Physiol*, **228**, 1873-1883.

50. Tartey, S., Matsushita, K., Vandenbon, A., Ori, D., Imamura, T., Mino, T., Standley, D.M., Hoffmann, J.A., Reichhart, J.M., Akira, S. *et al.* (2014) Akirin2 is critical for inducing inflammatory genes by bridging I kappa B-zeta and the SWI/SNF complex. *Embo J*, **33**, 2332-2348.

51. Pasparakis, M., Luedde, T. and Schmidt-Supprian, M. (2006) Dissection of the NF-kappaB signalling cascade in transgenic and knockout mice. *Cell Death Differ*, **13**, 861-872.

Chapter 2: Functional characterization and efficient detection of Nucleophosmin/NPM1 oligomers

2-1. Abstract

NPM1/nucleophosmin is a multifunctional phosphoprotein that has been implicated in oncogenesis. Plenty of observations have suggested that changes of the oligomer formation of NPM1 could influence its biological functions, especially its oncogenic functions, although the effect of oligomer formation on the biochemical activities of NPM1 is not well understood. This highlights the importance of monitoring the cellular oligomeric state of NPM1 under different conditions or stimuli for understanding its oncogenic functions. In this study, I demonstrate that oligomerization of NPM1 is necessary for its histone chaperone activity *in vitro*. Furthermore, to monitor the cellular oligomer formation of NPM1, I utilized the split synthetic *Renilla* luciferase protein fragment-assisted complementation (SRL-PFAC) bioluminescence and observed the change of NPM1 oligomer levels upon mitotic synchronization, TNF-α treatment, and serum starvation. This study provides a promising method for systematic characterization of NPM1 oligomer formation changes, and for screening of NPM1 oligomerization inhibitors for cancer therapy.

2-2. Introduction

NPM1/nucleophosmin/B23 was first identified as a phosphoprotein expressed at high levels in the granular region of the nucleolus [1]. It mainly resides in the nucleolus but continuously shuttles between the nucleolus, the nucleoplasm, and the cytoplasm [2]. It has been implicated in multiple cellular functions, including ribosome biogenesis [3], centrosome duplication [4], molecular chaperoning [5], chromatin regulation [6], and regulation of the ARF, HDM2, and p53 tumor suppressor pathway [7-9]. NPM1 directly binds to histones and mediates nucleosome assembly in vitro as a histone chaperone [6]. In addition, NPM1 binds directly to RNAs and the RNA binding activity of NPM1 is suggested to be required for its nucleolar localization [10]. Importantly, the genetic alterations of the NPM1 gene have been detected in hematological malignancies, and NPM1 overexpression was observed in various solid tumors. In addition to the overexpression of NPM1 protein and mutation of *NPM1* gene, NPM1 oligomerization has been suggested to maintain its oncogenic functions. All in all, NPM1 has been proposed as a cancer marker and potential therapeutic target for cancer therapy [11].

NPM1 belongs to the nucleoplasmin protein family which includes NPM2 and NPM3. All these proteins share a conserved N-terminal core domain that is required for oligomerization [12]. Various observations have suggested that the oligomeric state of NPM1 is important for its biological functions, especially its functions in cancer. For example, inhibition of NPM1 oligomerization by a small molecule [13] or an RNA aptamer [14] resulted in mislocalization of NPM1 in the nucleoplasm, induction of p53-dependent apoptosis, increased sensitivity to DNA damage in human cancer cells; IKKα promotes the oligomerization of NPM1 to induce the localization of NPM1 to centrosome, thereby maintains genome integrity [15]; cleavage of the NPM1 protein by the cytotoxic lymphocyte granule protease granzyme B in hepatoma but not normal liver cells stabilizes the oligomeric form of NPM1 to enhance the localization of NPM1 to the nucleolus [16]. The oligomerization of the N

terminal core domain of NPM1 is regulated by both posttranslational modification and protein binding. Phosphorylation in the N terminus of NPM1 destabilizes the oligomeric form of NPM1, while binding to target proteins containing R-rich motifs stabilizes the oligomeric structure, counteracting the destabilization associated with phosphorylation [16]. Given the importance of NPM1 oligomerization for its biological functions, it is important to monitor the changes of cellular NPM1 oligomeric state under different conditions or stimuli to understand its functions.

In this study, I first demonstrated that oligomerization of NPM1 is necessary for its histone chaperone activity, but dispensable for its binding to histones or RNA in vitro. To systematically monitor the cellular oligomer formation of NPM1, I utilized the split synthetic Renilla luciferase protein fragment-assisted complementation (SRL-PFAC) and examined the change of NPM1 oligomer levels under several cell culture conditions. This study provides a promising method for systematic characterization of NPM1 oligomer formation changes, and for screening of NPM1 oligomerization inhibitors.

2-3. Materials and methods

2-3-1. Cell culture, transfection, reporter assay, and reagents

HeLa and 293T cells were cultured in DMEM supplemented with 10% heat-inactivated fetal bovine serum (FBS) at 37ºC with 5% CO_2. To establish stable cell lines, HeLa cells were co-transfected with pcDNA3.1-Flag-N-RL-NPM1 and pcDNA3.1-Flag-C-RL-NPM1 or pcDNA3.1-Flag-N-RL-NPM1 and pcDNA3.1-Flag-C-RL using Gene Juice

(Novagen) according to the manufacturer's instructions. Neomycin-resistant cells were selected by 0.1 mg/ml G418.

Luciferase assay was performed using *Renilla* Luciferase Assay System kit (Promega Corporation, USA) according to the manufacturer's instructions. For mitotic cell preparation, cells were treated with 100 ng/ml Nocodazole for 18 h and mitotic cells were collected by gentle shaking of the dishes.

Antibodies used were NPM1 (FC-61991, Thermo Fisher Scientific), Flag-tag (M2, Sigma Aldrich), p65 (ab7970, Abcam) and β-actin (sc-47778, Santa Cruz Biotechnology). Recombinant human TNF-α (PEPROTECH) was commercially available.

2-3-2. Plasmid construction

To construct pET14b-NPM1-LG and -SG, cDNA fragments containing mutations were amplified by two-step PCR. First PCR was conducted using primers; 5'-TAATACGACTCACTATAGG-3' and 5'-AATATGCACTGGCCCTGAGGCACACTTGGCCCTTA-3', and 5'-CCACCAGTGGTCTTAAGGGCCAAGTGTGCCTCAGG-3' and 5'-GCTAGTTATTGCTCAGCGG-3' for pET14b-NPM1-LG, and 5'-TAATACGACTCACTATAGG-3' and 5'-AATATGCACTGGAGCAGCACCACACTTCAACCTTA-3', and 5'-TTGAAGTGTGGTGCTGCTCCAGTGCATATTAGTGG-3' and 5'-GCTAGTTATTGCTCAGCGG-3' for pET14b-NPM1-SG with pET14b-NPM1 as a template. These two fragments were purified and used as templates of second PCR and the full-length cDNA fragments were amplified using T7 promoter and terminator primers. The cDNA fragments were digested with Nde I and BamH I and inserted into the same sites of pET14b. For constructing pEGFP-Flag-NPM1-LG and -SG, pET14b-NPM1-LG and -SG were digested with Nde I and Hind III and cloned into the same sites of pBS-Flag. The pBS-Flag plasmids were digested with BamH I and then the cDNA for the

Flag-tagged proteins were cloned into BamH I digested pEGFP-C1.

For the split synthetic *Renilla* luciferase (hRL) fusion plasmids [17], the N-terminal (N-RL, a.a. 1-229) and C-terminal (C-RL, a.a. 230-311) synthetic *Renilla* luciferase gene were PCR-amplified using the primers containing the linker DNA sequences GGTGGCGGAGGGAGCGGTGGCGGAGGGAGC in the reverse primers. The N-RL and C-RL fragments were first PCR-amplified using phRL-TK (Promega) as a template with primers 5'-AGCTAGCATATGAATGGCTTCCAAGGTGTACGA-3' and 5'-ATGCGGATCCGCTCCCTCCGCCACCGCTCCCTCCGCCACCGCCTCCC TTAACGAGAGGGA-3' for N-RL, 5'-AGCTAGCATATGAAAGCCCGACGTCGTCCAGATT-3' and 5'-ATGCGGATCCGCTCCCTCCGCCACCGCTCCCTCCGCCACCCTGCTCG TTCTTCAGCACGC-3' for C-RL. All the amplified fragments were digested with Nde I and BamH I and subcloned into the same sites of pET14b to construct plasmids pET14b-N-RL and pET14b-C-RL plasmids. The cDNA for NPM1 was inserted to the BamH I site of pET14b-N-RL and pET14b-C-RL to construct pET14b-N-RL-NPM1 and pET14b-C-RL-NPM1. To construct pcDNA3.1-Flag-N-RL-NPM1, pcDNA3.1-Flag-C-RL-NPM1, and pcDNA3.1-Flag-C-RL, the cDNAs for N-RL-NPM1, C-RL-NPM1, and C-RL were PCR-amplified using pET14b vectors as templates with primers 5'-AGCTAGGAATTCAATGGCTTCCAAGGTGTACGA-3' and 5'-AGCTTCTAGATTAAAGAGACTTCCTCCACTGCCA-3', 5'-AGCTAGGAATTCAAAGCCCGACGTCGTCCAGATT-3' and 5'-AGCTTCTAGATTAAAGAGACTTCCTCCACTGCCA-3', and 5'-AGCTAGGAATTCAAAGCCCGACGTCGTCCAGATT-3' and 5'-ATGCTCTAGATTAGCTCCCTCCGCCACCGCTCCC-3', respectively. All the amplified fragments were digested with EcoR I and Xba I, and subcloned into the same sites of pcDNA3.1-Flag vector. All the amplified sequences were verified by DNA sequencing.

2-3-3. Binding assays

For immunoprecipitation assay, cells were lysed and sonicated in buffer A containing 150 mM NaCl and the supernatants were collected and mixed with ANTI-FLAG® M2 affinity gel (SIGMA-ALDRICH) followed by incubation at 4°C for 1 h. The Flag-tagged proteins were eluted with FLAG peptide (SIGMA-ALDRICH) after extensive washing and analyzed by SDS-PAGE followed by western blotting.

For GST-pull down assay, glutathione-sepharose beads immobilized GST proteins were mixed with 1 g of H2A-H2B or H3-H4 histone complexes in buffer A containing 100 mM NaCl and incubated at 4ºC for 2 h followed by extensive washing with the same buffer. Proteins were eluted from the beads with a SDS sample buffer, separated by SDS-PAGE, and visualized by CBB staining. Recombinant proteins and core histones were purified as described previously [18, 19].

2-3-4. Immunofluorescence

HeLa cells were treated without or with TNF-α (20 ng/ml) for 3 h, cells on cover slips were fixed with 3% paraformardehyde in PBS, and permeabilized in PBS containing 0.5% Triton X-100. The cells on coverslips were then incubated with p65 antibody diluted with PBS containing 0.5% non-fat dry milk. Localization of proteins was visualized with secondary antibodies conjugating with AlexaFluor dyes (Molecular Probes). During final wash with PBS containing 0.1% Triton X-100, DAPI DNA staining dye was added and incubated for 15 min at room temperature. Images were observed under confocal microscope (LSM EXCITER; Carl Zeiss Microimaging, Inc.).

2-3-5. Nucleosome assembly assay and RNA binding assay

Purified recombinant core histones (30 ng) were incubated with increased

amount of His-NPM1, His-NPM1-SG or His-NPM1-LG at room temperature for 20 min, followed by additional incubation with the 196 bp-long 5S rDNA fragment (10 ng) at room temperature for 30 min. Samples were resolved on a 6% native PAGE in 0.5xTBE buffer. DNA was visualized by GelRed staining.

Supercoiling assay was performed as described previously [6] using pCAGGS relaxed by incubation with topoisomerase I (TAKARA). Filter binding assay and sucrose density gradient assay were performed as described previously [18]. Total RNAs extracted from HeLa cells were labeled with polynucleotide kinase (TOYOBO) and [γ-^{32}P]ATP and used for filter binding assays.

2-4. Results

2-4-1. Biochemical characterization of NPM1 oligomers

To examine the effect of oligomerization of NPM1 on its biochemical activities, I have constructed NPM1 mutants that show low oligomerization activity. Previous study demonstrated that the mutations in amino acids L102, G105, S106, and G107 located in the GSGP loop in the oligomerization domain of NPM1 destabilize the oligomerization [20]. When the wild type NPM1 tagged with EGFP-Flag was expressed and immunoprecipitated, the endogenous NPM1 protein was co-immunoprecipitated (Fig. 1A, lanes 5 and 6), indicating the oligomerization of the exogenous and endogenous NPM1 proteins. On the other hand, NPM1-LG (L102A/G105A) and NPM1-SG (S106A/G107A) tagged with EGFP-Flag were immunoprecipitated with the endogenous NPM1 inefficiently (lanes 7 and 8). Therefore, these mutations were ensured to inhibit the oligomerization of NPM1.

To test the function of these oligomer mutants, the wild type and mutant proteins were expressed in *E. coli* and purified (Fig. 1C), and their histone chaperone activities and RNA binding activities were examined *in vitro*. I first examined the histone binding activities of NPM1 wild type and mutants by GST-pull down assays. GST-tagged wild type NPM1, but not GST alone, efficiently pulled down both the core histones H2A-H2B and H3-H4 complexes (Fig. 1B, lanes 1, 2, 5, and 6). Similarly, both GST-NPM1-SG and GST-NPM1-LG efficiently bound to core histones as did wild type (lanes 3, 4, 7, and 8), indicating that the oligomerization was dispensable for the histone binding activity of NPM1. Next, the nucleosome assembly activities of the mutants were examined using purified core histones and the 196 bp-long 5S rDNA fragment (Fig. 1D). When core histones were directly mixed with naked DNA, histones randomly bound to DNA and that the complex could not enter native PAGE (lanes 2, 6, and 10). However, when core histones were preincubated with wild type NPM1 and then DNA was added, the bands

migrated slower than naked DNA appeared. These bands were previously shown to correspond to nucleosome core particle [19], suggesting that wild type NPM1 binds to core histones and transfer them to naked DNA to assemble a nucleosome core particle. On the other hand, the activities of NPM1-LG and NPM1-SG were much less than that of wild type (lanes 7–9 and 11–13). To further confirm the activity of the oligomer mutant proteins, supercoiling assay was performed using purified histones and relaxed circular plasmid DNA. When nucleosome structure is formed on plasmid in the presence of topoisomerase I, negative supercoil is introduced in the plasmid DNA (Form II), which migrates faster than relaxed circular DNA (Form I). When core histones alone were mixed with plasmid DNA, supercoil was not introduced. When core histones preincubated with increasing amounts of NPM1 were mixed with plasmid, Form II plasmid DNA was increased with increasing amount of NPM1, suggesting that NPM1 mediates efficient nucleosome assembly. On the other hand, the nucleosome assembly activities of NPM1-LG and NPM1-SG were not detected by supercoiling assay. These results indicate that the oligomerization of NPM1 is dispensable for histone binding but essential for the nucleosome assembly activity *in vitro*.

I next examined the RNA binding activity of NPM1 *in vitro*. NPM1 binds to RNA through the C-terminal globular domain (Fig. 2A). The RNA binding activity of the NPM1 proteins were examined by filter binding assay using [^{32}P]-labeled RNAs. Wild type NPM1 bound to RNAs in a dose-dependent manner and labeled RNA was retained on the membrane (Fig. 2B). NPM1-LG also bound to RNA with similar efficiency with wild type NPM1, suggesting that the oligomerization state of NPM1 did not strongly affect its RNA binding activity *in vitro*. I have previously shown that NPM1 binds to ribosomal RNAs and shows binding preference to 28S rRNAs [18]. To determine whether the oligomerization of NPM1 affects the RNA biding preference, sucrose density gradient assays were performed (Fig. 2C). Wild type NPM1 was

co-fractionated preferentially with 28S rRNA, whereas B23.2, a splicing variant of NPM1, lacking the RNA binding domain was recovered in top fractions. I demonstrated that NPM1-LG was co-fractionated preferentially with 28S rRNA as did wild type NPM1. These results indicated that the oligomerization of NPM1 is dispensable for the RNA binding activity *in vitro*.

2-4-2. Establishment of the detection system of NPM1 oligomers

Given the reported importance of NPM1 oligomerization for its biological functions and the different biochemical activities between the NPM1 monomer and oligomers, I next aimed to establish the detection system of the NPM1 oligomers. I applied the split synthetic *Renilla* luciferase (RL) protein fragment-assisted complementation (SRL-PFAC) bioluminescence system [17] to detect the NPM1 oligomers. NPM1 was fused to the N-terminal RL (N-RL, a.a. 1–229) and C-terminal RL (C-RL, a.a. 230–311) proteins through a $(Gly_4Ser)_2$ peptide linker (Fig. 3A). The oligomerization of NPM1 will bring N-RL and C-RL in close proximity and lead to complementation of the RL enzyme activity. I first tested this system by transiently co-transfection of N-RL-NPM1 with C-RL-NPM1 or C-RL in 293T cells and reporter assay was performed (Figs. 3B and C). Cells transiently expressing N-RL-NPM1 and C-RL-NPM1 showed dramatically higher luciferase activity than that in control cells expressing N-RL-NPM1 and C-RL, indicating that N-RL-NPM1 formed an oligomer with C-RL-NPM1 but not C-RL in the cells. To systematically study the oligomerization of NPM1 in the cells, I established HeLa cell lines stably expressing N-RL-NPM1 and C-RL-NPM1 or N-RL-NPM1 and C-RL (Fig. 3D). The luciferase activity of the cell line expressing N-RL-NPM1 and C-RL-NPM1 showed significantly higher luciferase activity than that of the control cell line expressing N-RL-NPM1 and C-RL, and was increased in a cell number dependent manner, indicating that the cell lines were successfully established and could be used for further study of NPM1 oligomerization in the cells.

2-4-3. Detection of cellular NPM1 oligomerization levels upon various stimuli

I first applied this assay system for the detection of NPM1 oligomerization state in TNF-α treated cells, because oligomerization of NPM1 is promoted by the phosphorylation at Ser125 by IKKα that is activated by TNF-α stimulation [15]. Upon TNF-α treatment, the p65 subunit of Nuclear Factor-κB was translocated into the nucleus (Fig. 4A), indicating the activation of IKKα by TNF-α in HeLa cells. Upon TNF-α treatment, the luciferase activity in the cells expressing N-RL-NPM1 and C-RL-NPM1 was increased in a time-dependent manner, whereas that in cells expression N-RL-NPM1 and C-RL was unchanged, indicating that TNF-α treatment enhanced the oligomerization of NPM1. Given that the oligomer formation of NPM1 was affected by the phosphorylation at the site (Ser125) outside of the oligomerization domain upon TNF-α treatment, it was speculated that the phosphorylation at the unstructured region affect the oligomerization state of NPM1. To test this speculation, I analyzed the NPM1 oligomerization state during the cell cycle. NPM1 is phosphorylated at sites outside of the oligomerization domain by mitotic kinases [10, 21, 22]. The cells were synchronized at mitosis by nocodazole treatment (Figs. 4C and D) or at G0/G1 phase by serum starvation (Figs. 4E and F), and the luciferase activity of the cells was examined. The same number of asynchronous and mitotic cells was collected for western blotting and luciferase assays. The expression of cyclin B in mitotic cells was much stronger than that in asynchronous cells, whereas the expression of N-RL-NPM1 and C-RL-NPM1 was not changed (Figs. 4C and E). Interestingly, the luciferase activity in mitotic cells showed significantly higher activity than that in asynchronous cells (Fig. 4D). I also found that the luciferase activity was decreased upon serum starvation in (Fig. 4F), indicating that the NPM1 oligomers was decreased upon serum starvation. These results indicate that NPM1 oligomerization state is changed during the cell cycle. In addition, the

assay system using the SRL-PFAC is demonstrated to be a useful tool to monitor the NPM1 oligomerization state in the cells.

2-5. Figures and legends

Figure 1

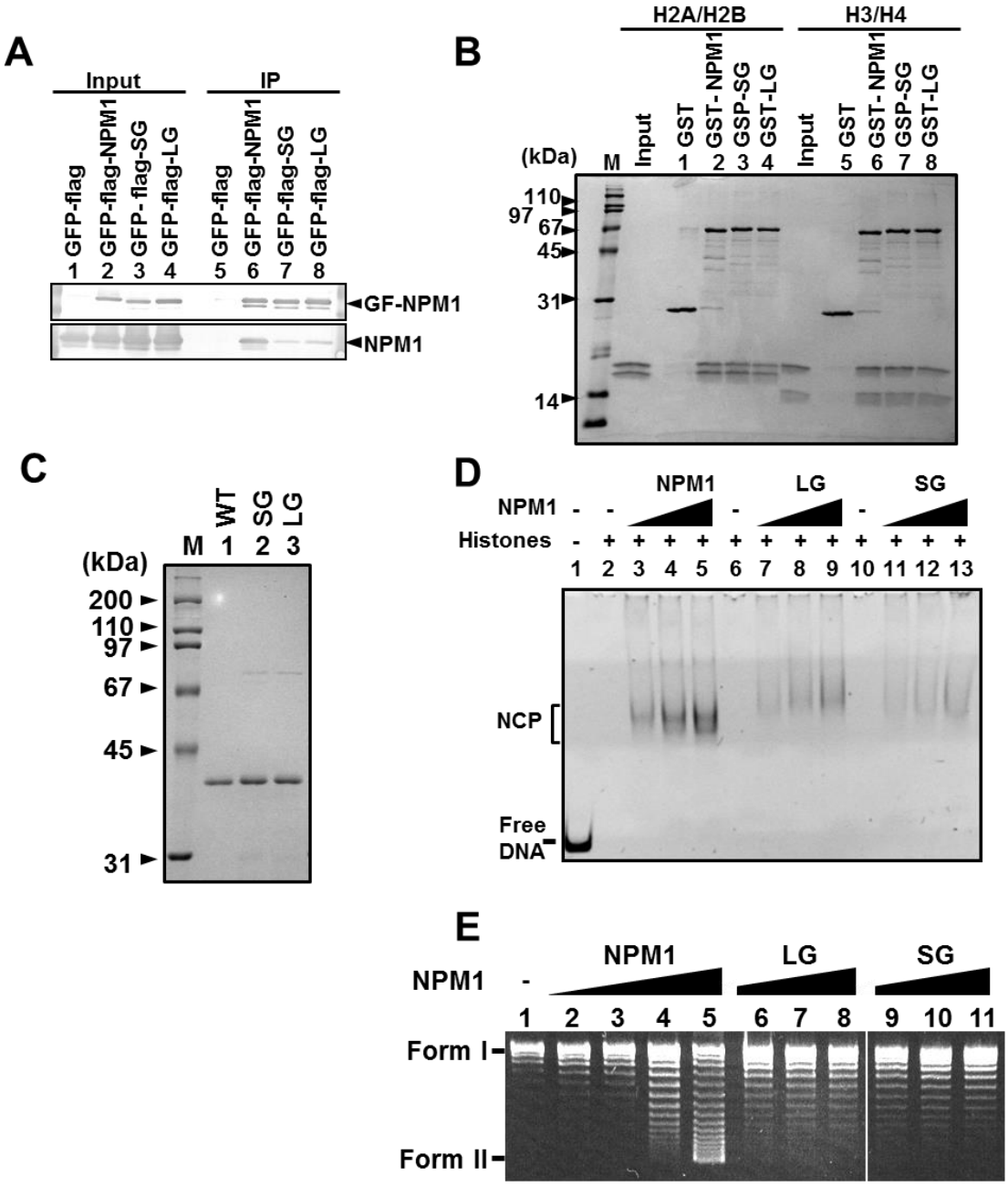

Fig.1 Histone chaperone activity of NPM1 wild type and oligomer mutants

A. Immunoprecipitation. GFP-Flag (GF), GFP-Flag-B23.1-Wt, -LG, or -SG was transiently expressed in 293T cells, the GFP-Flag-tagged proteins were immunoprecipitated with Anti-FLAG M2 Affinity Gel, and input and immunoprecipitated proteins were analyzed by SDS-PAGE followed by

western blotting using anti-NPM1 antibody. B. GST-pull down assay. Purified GST, GST-NPM1, -SG, and -LG were mixed with either recombinant H2A-H2B (lanes 1–4) or H3-H4 (lanes 5–8) complexes and GST-pull down assays were performed. The proteins were analyzed by 15% SDS-PAGE and visualized by Coomassie Brilliant Blue (CBB) staining. Inputs indicate recombinant histone proteins used for the assays. Lane M indicates molecular weight markers. C. Purified His-tagged NPM1 proteins. Purified His-tagged NPM1 wild type (wt), -SG, and -LG were separated by 10% SDS-PAGE and visualized by CBB staining. D. Histone transfer assay. Core histones (30 ng) were mixed with increasing amounts of His-tagged proteins (150, 300, and 600 ng), and then 196 bp-long DNA was added and further incubated. The complexes were loaded on 6% native PAGE and DNA was visualized by Gel Red staining. Positions of free DNA and nucleosome core particle (NCP) are indicated at the left side of the panel. E. Supercoiling assay. Increasing amounts of His-NPM1 (lanes 2–5; 150, 300, 600, and 1,200 ng), His-NPM1-SG and His-NPM1-LG (lanes 6–8 and 9–11; 300, 600, and 1,200 ng) mixed with core histones (200 ng) were incubated with relaxed plasmid DNA (200 ng) at 37^{o}C for 50 min in the presence of DNA topoisomerase I. Purified plasmid DNA was separated on 1% agarose gel and visualized by staining with Gel Red. Positions of relaxed (Form I) and supercoiled (Form II) plasmid DNA are shown at the left side of the panel.

Figure 2

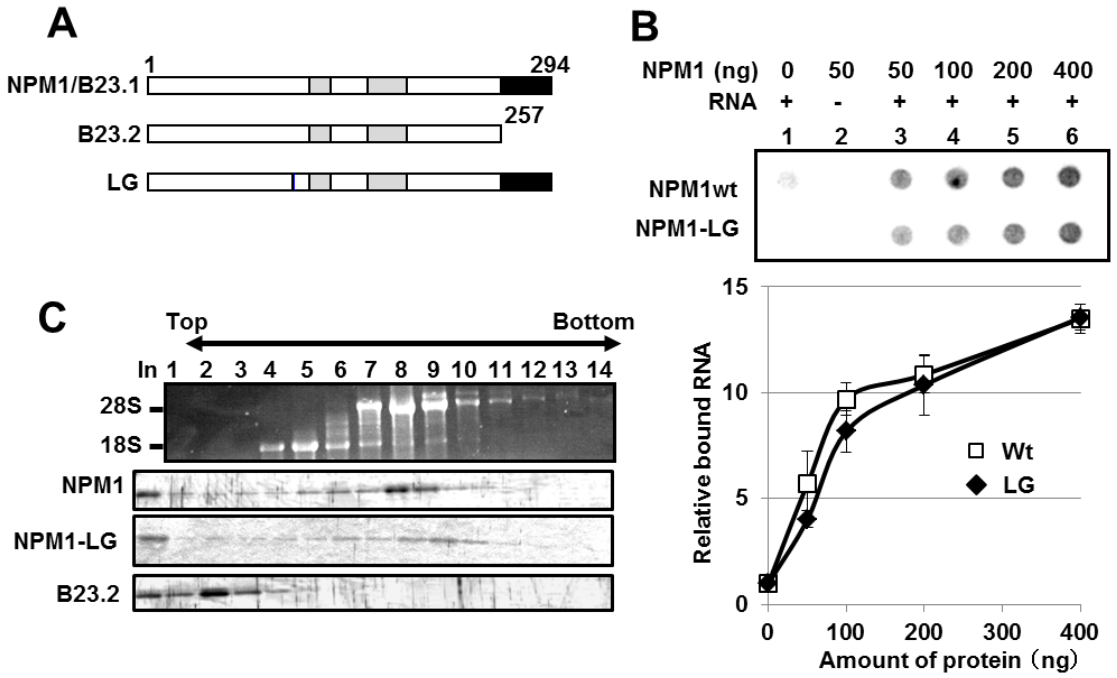

Fig. 2. Effect of NPM1 oligomerization on its RNA binding activity

A. Schematic representation of NPM1 and its mutants. Central acidic regions and the C-terminal RNA binding domain are shown with right gray and black, respectively. B. Filter binding assay. [^{32}P]-labeled RNA was incubated alone or with increasing amount of GST, GST-NPM1, or GST-NPM1-LG (50, 100, 200, and 400 ng). The amount of RNA remained on the nitrocellulose membrane were measured and the relative amount of RNA was plotted in the graph. B. Sucrose density gradient centrifugation assays. His-tagged NPM1 proteins (5 μg) were incubated with total RNA (10 μg) purified from HeLa cells at room temperature for 30 min and separated on 15%–45% sucrose gradient. The proteins in each fraction were analyzed by SDS-PAGE followed by silver staining. RNAs in each fraction were purified, separated on 1% denature agarose gel, and visualized by staining with GelRed. RNA data shown in the top panel is for NPM1 wild type.

Figure 3

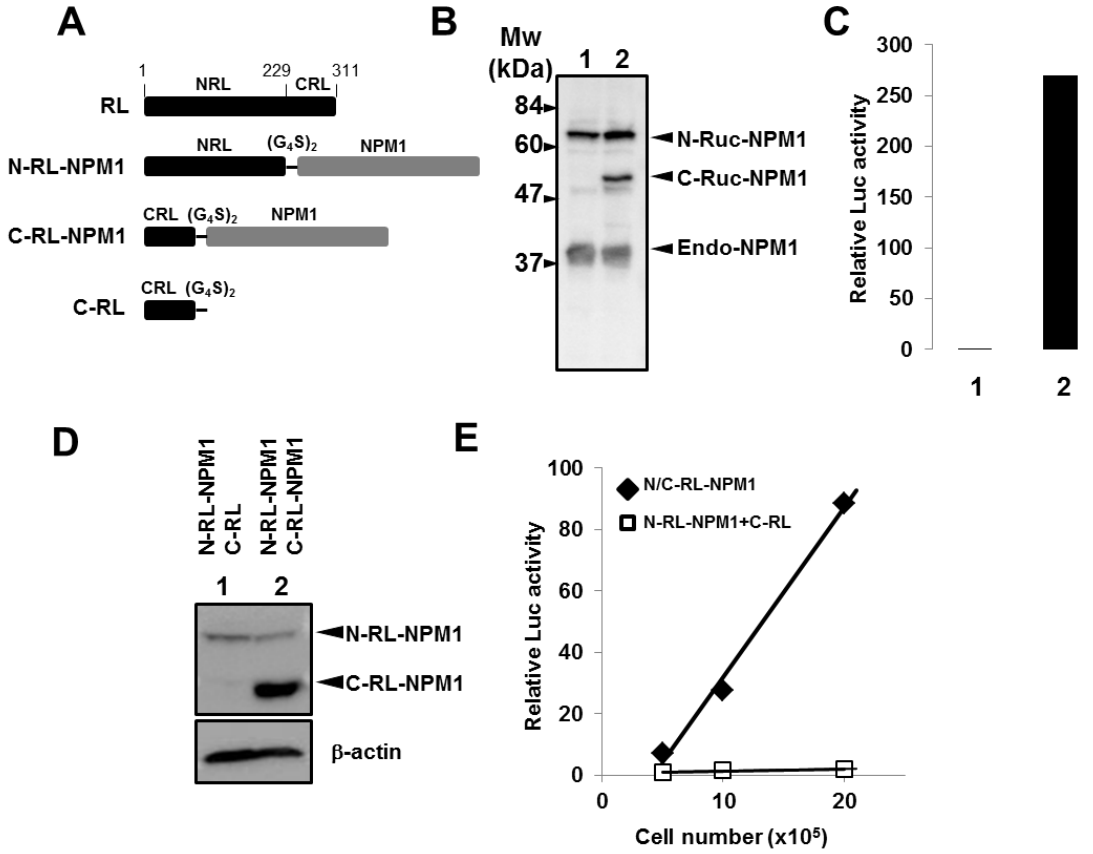

Fig. 3 Detection of the NPM1 oligomers by the split synthetic *Renilla* luciferase (RL) fragment-assisted complementation

A. Schematic diagram for the chimeric proteins. NPM1 was fused to the N-RL (amino acids 1-229) and C-RL (amino acids 230-311) portion of the RL through an $(G_4S)_2$ peptide linker. B, C. Detection of NPM1 oligomer by SRL-PFAC using transiently transfected cells. N-RL-NPM1 and C-RL-NPM1, or N-RL-NPM1 and C-RL were transiently expressed in HeLa cells and the expression of the proteins were examined by western blotting with anti-NPM1 antibody. In parallel, luciferase assays were performed and relative luciferase activity (the activity in control cell was set as 1.0) was calculated and shown in C. D. Construction of HeLa cell line stably expressing Flag-N-RL-NPM1 and Flag-C-RL-NPM1, or Flag-N-RL-NPM1 and Flag-C-RL. Expression of proteins were detected by anti-NPM1 antibody (D). Flag-C-RL was too small to be

detected. β-actin was also detected as a control. Luciferase activities of different cell numbers from each cell line were examined and relative luciferase activity was plotted in E.

Figure 4

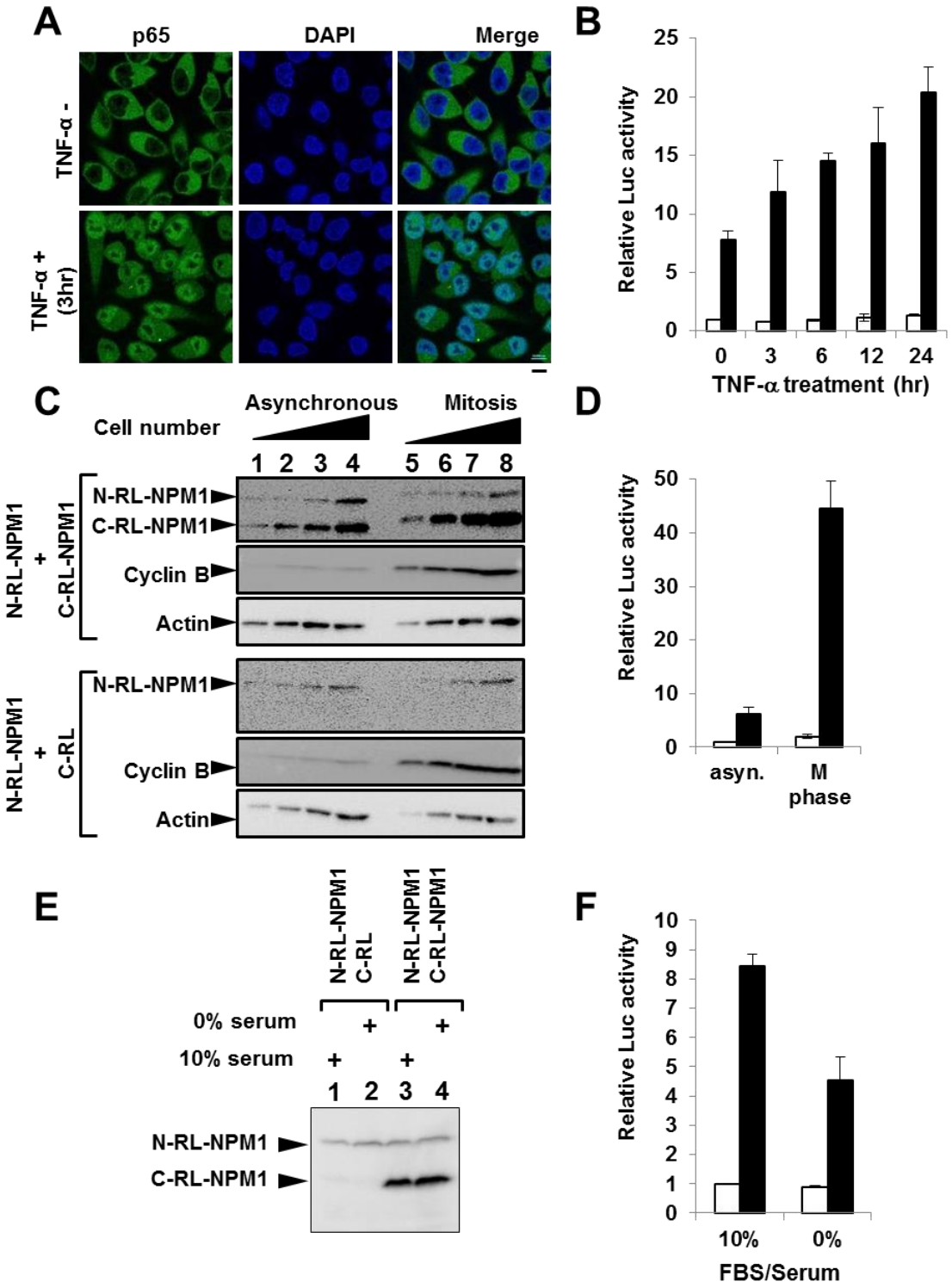
A
p65
DAPI
Merge
TNF-α -
TNF-α + (3hr)
B
Relative Luc activity
25
20
15
10
5
0
0 3 6 12 24
TNF-α treatment (hr)
C
Asynchronous
Mitosis
Cell number
1 2 3 4 5 6 7 8
N-RL-NPM1 + C-RL-NPM1
N-RL-NPM1
C-RL-NPM1
Cyclin B
Actin
N-RL-NPM1 + C-RL
N-RL-NPM1
Cyclin B
Actin
D
Relative Luc activity
50
40
30
20
10
0
asyn.
M phase
E
N-RL-NPM1 C-RL
N-RL-NPM1 C-RL-NPM1
0% serum
10% serum
1 2 3 4
N-RL-NPM1
C-RL-NPM1
F
Relative Luc activity
10
9
8
7
6
5
4
3
2
1
0
10%
0%
FBS/Serum

Fig. 4 Change of NPM1 oligomerization state under various cell culture conditions

A. Localization of the p65 subunit of NF-κB in HeLa cells treated without or with TNF-α. HeLa cells were treated with TNF-α (20 ng/ml) and localization of p65 was examined with anti-p65 antibody. DNA was visualized with DAPI staining. Scale bar indicates 10 m. B. Effect of TNF-α treatment on the oligomerization of NPM1. HeLa cells stably expressing N-RL-NPM1/C-RL-NPM1 and N-RL-NPM1/C-RL were treated with TNF-α (20 ng/ml) for 3–24 hours and luciferase activity of the cells were examined. C, D Oligomeric state of NPM1 in asynchronous and mitotic cells. Asynchronous and mitotic cell lines were prepared and the expression of NPM1 proteins, Cyclin B, and -actin were detected by western blotting. In parallel, luciferase activities of the cells were examined and shown in D. E, F. Effect of serum starvation on the oligomerization of NPM1. The cell lines were incubated in medium contains 0% or 10% FBS for 28 h, and the expression of NPM1 proteins were detected by western blotting and the luciferase activity was detected (F). For the graph in B, D, and F, blank and filled bars indicate the luciferase activity for cell line expressing N-RL-NPM1/C-RL and N-RL-NPM1/C-RL-NPM1, respectively. Three independent experiments were performed and error bars indicate ±SD.

2-6. Discussion

Various observations have suggested that changes in the oligomeric state of NPM1 may influence its biological functions and subcellular localization [23]. However, the biochemical function of the oligomerization has been poorly understood. In this study, I demonstrated that the oligomerization of NPM1 is required for its histone chaperone activity. Thus, it is suggested that the histone chaperone function of NPM1 is regulated by monomer-oligomer conversion. The nucleolar localization of NPM1 requires its biding to RNA [24], and monomeric NPM1 is mainly localized in the nucleoplasm [14], raising the possibility that the nucleoplasmic NPM1 may lose its RNA binding activity. However, my *in vitro* result showed that the monomeric and oligomeric NPM1 showed similar RNA binding activity, indicating that the nucleoplasmic localization of NPM1 monomer is not caused by loss of RNA binding activity. The nucleoplasmic localization of NPM1 monomer may be caused by posttranscriptional modifications, interaction with nucleoplasmic proteins, or loss of interaction with nucleolar proteins.

I also established an assay to systematically study the cellular oligomerization of NPM1 using the split synthetic *Renilla* luciferase protein. By using this assay I examined the cellular oligomerization state of NPM1 under different cell culture conditions or stimuli. It was reported that IKKα promotes the oligomerization of NPM1 to induce the localization of NPM1 to centrosome, thereby maintains genome integrity, and prevents tumor progression [15] Consistent with the previous report, my result showed that TNF-α treatment that activated the IKKα enhanced the oligomerization of NPM1. This result ensures the usefulness of the assay system. Furthermore, I also examined the oligomerization of mitotic NPM1 of which cellular localization is dramatically changed [25]. My result showed that mitotic NPM1 shows much higher oligomer level compared with interphase NPM1. This may be resulted from the phosphorylation of NPM1 during mitosis. Phosphorylations of NPM1 have

been reported to affect the functions of NPM1. For example, NPM1 associates with unduplicated centrosomes and dissociates from centrosome to allow its duplication upon phosphorylation at Thr199 by CDK2/cyclin E during G1 phase [15]; phosphorylation of NPM1 during mitosis by cyclin B/Cdc2 inactivates the RNA binding of NPM1 resulted the release of NPM1 from chromatin [24, 26]. I also showed that serum starvation that can cause the translocation of NPM1 from the nucleolus to the nucleoplasm [27] decreases the oligomerization of NPM1, this may be caused by posttranslational modifications such as phosphorylation, or loss of the interaction with R-rich motif containing proteins since interaction with R-rich motif containing protein can promote its nucleolar localization [23]. Although the biological significance of enhanced oligomer formation in mitosis is not clear, the decreased oligomer formation of NPM1 in serum starved cells is likely to contribute to the inhibition of ribosome biogenesis by excluding NPM1 from the nucleoli.

These successful detections of changes of NPM1 oligomerization under different cell culture conditions suggest that this assay system can be used for systematically study the cellular oligomerization of NPM1 under various conditions to understand the functions of NPM1. Moreover, it can also be a promising method for the screening of NPM1 oligomerization inhibitor for cancer therapy.

2-7.

2-8. Reference

[1] Y.J. Kang, M.O. Olson, C. Jones, H. Busch, Nucleolar phosphoproteins of normal rat liver and Novikoff hepatoma ascites cells, Cancer Res, 35 (1975) 1470-1475.

[2] R.A. Borer, C.F. Lehner, H.M. Eppenberger, E.A. Nigg, Major nucleolar proteins shuttle between nucleus and cytoplasm, Cell, 56 (1989) 379-390.

[3] D. Chen, S. Huang, Nucleolar components involved in ribosome biogenesis cycle between the nucleolus and nucleoplasm in interphase cells, J Cell Biol, 153 (2001) 169-176.

[4] M. Okuda, H.F. Horn, P. Tarapore, Y. Tokuyama, A.G. Smulian, P.K. Chan, E.S. Knudsen, I.A. Hofmann, J.D. Snyder, K.E. Bove, K. Fukasawa, Nucleophosmin/B23 is a target of CDK2/cyclin E in centrosome duplication, Cell, 103 (2000) 127-140.

[5] A. Szebeni, M.O. Olson, Nucleolar protein B23 has molecular chaperone activities, Protein Sci, 8 (1999) 905-912.

[6] M. Okuwaki, K. Matsumoto, M. Tsujimoto, K. Nagata, Function of nucleophosmin/B23, a nucleolar acidic protein, as a histone chaperone, Febs Lett, 506 (2001) 272-276.

[7] S. Kurki, K. Peltonen, L. Latonen, T.M. Kiviharju, P.M. Ojala, D. Meek, M. Laiho, Nucleolar protein NPM interacts with HDM2 and protects tumor suppressor protein p53 from HDM2-mediated degradation, Cancer Cell, 5 (2004) 465-475.

[8] E. Colombo, J.C. Marine, D. Danovi, B. Falini, P.G. Pelicci, Nucleophosmin regulates the stability and transcriptional activity of p53, Nat Cell Biol, 4 (2002) 529-533.

[9] K. Itahana, K.P. Bhat, A. Jin, Y. Itahana, D. Hawke, R. Kobayashi, Y. Zhang, Tumor suppressor ARF degrades B23, a nucleolar protein involved in ribosome biogenesis and cell proliferation, Mol Cell, 12 (2003) 1151-1164.

[10] M. Okuwaki, M. Tsujimoto, K. Nagata, The RNA binding activity of a ribosome biogenesis factor, nucleophosmin/B23, is modulated by phosphorylation with a cell cycle-dependent kinase and by association with its subtype, Mol Biol Cell, 13 (2002) 2016-2030.

[11] E. Colombo, M. Alcalay, P.G. Pelicci, Nucleophosmin and its complex network: a possible therapeutic target in hematological diseases, Oncogene, 30 (2011) 2595-2609.

[12] M. Okuwaki, The structure and functions of NPM1/Nucleophsmin/B23, a multifunctional nucleolar acidic protein, J Biochem, 143 (2008) 441-448.

[13] W. Qi, K. Shakalya, A. Stejskal, A. Goldman, S. Beeck, L. Cooke, D. Mahadevan, NSC348884, a nucleophosmin inhibitor disrupts oligomer formation and induces apoptosis in human cancer cells, Oncogene, 27 (2008) 4210-4220.

[14] Y. Jian, Z. Gao, J. Sun, Q. Shen, F. Feng, Y. Jing, C. Yang, RNA aptamers interfering with nucleophosmin oligomerization induce apoptosis of cancer cells, Oncogene, 28 (2009) 4201-4211.

[15] X. Xia, S. Liu, Z. Xiao, F. Zhu, N.Y. Song, M. Zhou, B. Liu, J. Shen, K. Nagashima, T.D. Veenstra, S. Burkett, M. Datla, J. Willette-Brown, H. Shen, Y. Hu, An IKKalpha-nucleophosmin axis utilizes inflammatory signaling to promote genome integrity, Cell Rep, 5 (2013) 1243-1255.

[16] D.B. Ulanet, M. Torbenson, C.V. Dang, L. Casciola-Rosen, A. Rosen, Unique conformation of cancer autoantigen B23 in hepatoma: a mechanism for specificity in the autoimmune response, Proc Natl Acad Sci U S A, 100 (2003) 12361-12366.

[17] R. Paulmurugan, S.S. Gambhir, Monitoring protein-protein interactions using split synthetic renilla luciferase protein-fragment-assisted complementation, Anal Chem, 75 (2003) 1584-1589.

[18] M. Hisaoka, K. Nagata, M. Okuwaki, Intrinsically disordered regions of nucleophosmin/B23 regulate its RNA binding activity through their inter- and intra-molecular association, Nucleic Acids Res, 42 (2014) 1180-1195.

[19] M. Okuwaki, M. Abe, M. Hisaoka, K. Nagata, Regulation of cellular dynamics and chromosomal binding site preference of linker histones H1.0 and H1.X, Mol Cell Biol, (2016).

[20] T. Enomoto, M.S. Lindstrom, A. Jin, H. Ke, Y. Zhang, Essential role of the B23/NPM core domain in regulating ARF binding and B23 stability, J Biol Chem, 281 (2006) 18463-18472.

[21] H. Zhang, X. Shi, H. Paddon, M. Hampong, W. Dai, S. Pelech, B23/nucleophosmin serine 4 phosphorylation mediates mitotic functions of polo-like kinase 1, J Biol Chem,

279 (2004) 35726-35734.

[22] J. Shandilya, P. Senapati, K. Dhanasekaran, S.S. Bangalore, M. Kumar, A.H. Kishore, A. Bhat, G.S. Kodaganur, T.K. Kundu, Phosphorylation of multifunctional nucleolar protein nucleophosmin (NPM1) by aurora kinase B is critical for mitotic progression, Febs Lett, 588 (2014) 2198-2205.

[23] D.M. Mitrea, C.R. Grace, M. Buljan, M.K. Yun, N.J. Pytel, J. Satumba, A. Nourse, C.G. Park, M. Madan Babu, S.W. White, R.W. Kriwacki, Structural polymorphism in the N-terminal oligomerization domain of NPM1, Proceedings of the National Academy of Sciences of the United States of America, 111 (2014) 4466-4471.

[24] M. Okuwaki, M. Tsujimoto, K. Nagata, The RNA binding activity of a ribosome biogenesis factor, nucleophosmin/B23, is modulated by phosphorylation with a cell cycle-dependent kinase and by association with its subtype, Mol Biol Cell, 13 (2002) 2016-2030.

[25] O.V. Zatsepina, I.T. Todorov, R.N. Philipova, C.P. Krachmarov, M.F. Trendelenburg, E.G. Jordan, Cell cycle-dependent translocations of a major nucleolar phosphoprotein, B23, and some characteristics of its variants, European journal of cell biology, 73 (1997) 58-70.

[26] M. Hisaoka, S. Ueshima, K. Murano, K. Nagata, M. Okuwaki, Regulation of nucleolar chromatin by B23/nucleophosmin jointly depends upon its RNA binding activity and transcription factor UBF, Mol Cell Biol, 30 (2010) 4952-4964.

[27] P.K. Chan, M. Aldrich, H. Busch, Alterations in immunolocalization of the phosphoprotein B23 in HeLa cells during serum starvation, Experimental cell research, 161 (1985) 101-110.

Chapter 3: Summary, significance and perspective

NPM1 is a multi-functional protein that might contribute to tumorigenesis in different ways. This dissertation describes the mechanisms underlying the oncogenic functions of NPM1 in different aspects.

The first chapter is focused on the function of NPM1 in NF-κB pathway. I found that NPM1 contributes to the full activation of NF-κB by enhancing its DNA binding activity. NPM1 regulated NF-κB mediated inflammatory genes in both cancer cells and normal cells like macrophages suggest the oncogenic role of NPM1 in both tumor cells and the tumor microenvironment through the regulation of NF-κB. This result suggests that the oncogenic functions of NPM1 might result from the sum of comprehensive effect on both cancer cells and normal cells, emphasizing the importance of studying the oncogenic functions of NPM1 *in vivo* in future. The correlation between NPM1 expression and activation of NF-κB in colon and breast cancer, and its contribution to NF-κB activity suggests that the expression level of NPM1 is a suitable diagnostic marker to determine the aggressiveness of cancer cells and also a suitable target of cancer therapy. In addition to NF-κB, my microarray data showed that NPM1 might also regulate other transcription factors that regulate the cancer development (data not shown). Thus, it may be important to elucidate the interactome between NPM1 and the transcription factors and investigate whether there is a consensus mechanism underlying the regulation of transcription factors by NPM1.

The second project is focused on the study of NPM1 oligomerization. Plenty of observations have suggested that the implication of NPM1 oligomerization in cancer cells than that in normal cells, and inhibition of NPM1 oligomerization caused the apoptosis of cancer cells. However, the mechanism is still elusive. Here, I reported that the NPM1 oligomerization is required for its histone

chaperone activity. Previously, my laboratory reported that the histone chaperone activity of NPM1 regulated the ribosomal DNA (rDNA) gene transcription through regulation of the histone density on the rDNA gene promoters. Since NPM1 oligomerization is required for its histone chaperone activity, the oligomerization of NPM1 may be important for the ribosomal biogenesis to provide enough “energy” in cancer cells. Moreover, I successfully established the system for detection of dynamic NPM1oligomerization in the cell, which on the one hand, can be applied for examine the dynamic change of NPM1 oligomerization in different conditions for better understanding of the oncogenic functions of NPM1, on the other hand, it can also be used for screening of NPM1 oligomer inhibitors for cancer therapy.

This dissertation suggests the complex oncogenic functions of NPM1, which could be the regulation of transcription factor or ribosomal biogenesis, or other undiscovered mechanisms. Due to the multiple roles NPM1 plays in cancer, it may be the suitable target for cancer therapy.

Acknowledgements

I thank Dr. Emanuela Colombo (European Institute of Oncology, Italy) for her kind gifts of *p53*$^{-/-}$ and *p53*$^{-/-}$*NPM1*$^{-/-}$ MEFs, Dr. Kenkichi Masutomi (National Cancer Center Research Institute, Japan) for his gift of breast cancer cell lines, Dr. Yukari Okita (University of Tsukuba, Japan) for her help to maintain the *Apc*$^{min/+}$ mice and immunohistochemistry analyses, and Dr. Youqiong Ye for her help to analyze the microarray data using the software *R*. I also thank Professor Mitsuyasu Kato for kindly providing the *APC*$^{-/min}$ mice, and supervising the all the experiments using mice. I want to show many thanks to Dr, Miharu Hisaoka who equally contributed to this work (Chapter 2). I also thank Professor Kyosuke Nagata for supervising my whole project and discussing all my progress, Professor Mitsuru Okuwaki for designing the experiments with me, supervising all my experiments, and reviewing my manuscript.